Phosphorus starvation and luxury uptake in microalgae revisited

Alexei Solovchenko[1,7,8*], Inna Khozin-Goldberg[2], Irina Selyakh[1], Larisa Semenova[1], Tatiana Ismagulova,[1] Alexandr Lukyanov[1], Ilgar Mamedov[3], Ivan Zvyagin[3], Olga Gorelova,[1] Elizaveta Vinogradova[1], Olga Karpova[1], Ivan Konyukhov[1], Svetlana Vasilieva[1], Peter Mojzes[4], Cor Dijkema[5], Margarita Vecherskaya[5], Ladislav Nedbal[6].

[1]Department of Bioengineering, Faculty of Biology, Lomonosov Moscow State University, 1/12 Leninskie Gori, 119234 Moscow, Russia

[2]Shemyakin and Ovchinnikov Institute of Bioorganic Chemistry, Russian Academy of Sciences, 117997 Moscow, Russia

[3]Microalgal Biotechnology Laboratory, The French Associates Institute for Agriculture and Biotechnology for Drylands, The J. Blaustein Institutes for Desert Research, Ben-Gurion University of the Negev, Sede-Boqer Campus, Midreshet Ben-Gurion 84990, Israel

[4]Institute of Physics, Faculty of Mathematics and Physics, Charles University, Ke Karlovu 5, CZ-12116 Prague 2, Czech Republic

[5]Department of Biophysics, Wageningen University and Research Centre (WUR), Dreijenlaan 3, 6703 HA Wageningen, The Netherlands

[6]Institute of Bio- and Geosciences**/**Plant Sciences (IBG-2), Forschungszentrum Jülich**,** 52425 Jülich, Germany

[7]Michurin Federal Scientific Centre, Michurina 30, 393760 Michurinsk, Russia

[8]Peoples Friendship University of Russia (RUDN University), 117198 Moscow, Russia

*Corresponding author. Tel.: +7 495 939 25 87. E-mail address: solovchenko@mail.bio.msu.ru (A.E. Solovchenko).

Highlights

- P-starved *Chlorella vulgaris* cells re-fed with P_i transiently accumulated polyphosphate
- Polyphosphate accumulation is co-determined by P_i uptake and cell division rates
- P starvation reduces photosynthesis but exerts a modest effect on polar lipid composition
- Vacuolar PolyP granules display highly-ordered ultrastructural organization
- P-starvation and luxury uptake stages show distinct gene expression patterns

Abstract Phosphorus (P) is central to storing and transfer of energy and information in living cell including that of microalgae. Microalgae mostly dwell in low-P environments, so they are naturally equipped to take up and store P whenever it becomes available through a complex phenomenon known as 'luxury P uptake.' Knowing its mechanisms is a key to understanding of nutrient-driven rearrangements in natural microbial communities, control of industrial algal cultivation, and sustainable usage of P by its recycling from wastewater into biofertilizers. Here, we report on recent insights in luxury P uptake and polyphosphate formation originating from physiological, ultrastructural, and transcriptomic evidence. Special attention is paid to differential effects of P starvation and subsequent re-feeding on growth, P uptake, photosynthesis, changes in lipid and polyphosphate content and composition. The cultures pre-starved of P responded to feeding by inorganic phosphate by uptake that occurred in multiple phases and by formation of polyphosphate granules. P starvation impacted profoundly photochemistry but exerted only a moderate effect on cell lipid composition. The extent of polyphosphate accumulation was inversely related with the rates of cell division and P uptake resulting in a transient polyphosphate accumulation before the resumption of cell division. Electron microscopy studies revealed ordered organization of vacuolar deposits of polyphosphate indicative of possible involvement of an enzyme (complex) in their synthesis. A candidate gene was revealed encoding such an enzyme (a VTC-like protein) featuring an expression pattern corresponding to that of polyphosphate accumulation. Implications of the findings for efficient biocapture of phosphorus and generation of polyphosphate-enriched biomass suitable for conversion into biofertilizer are discussed.

Key words: Chlorella, luxury uptake, phosphorus starvation, lipids, polyphosphate, transcriptomics, photochemistry

Abbreviations: APF – acid purple phosphatase; Chl – chlorophyll; DDW – double-distilled water; DMSO – dimethyl sulfoxide; DW – dry weight; EDX – energy-dispersive X-ray; EPBR – Enhanced Phosphorus Bioremoval; FA – fatty acid(s); FAME–fatty acid methyl esters; GC-FID – gas chromatography with flame ionization detection; LD – lipid droplets; NMR – nuclear magnetic resonance; NPQ – non-photochemical quenching; P – phosphorus; P_i – inorganic phosphate; PHB – polyhydroxybutyrate; PolyP – inorganic polyphosphate; RTPCR – real-time polymerase chain reaction; TAG – triacylglycerol(s); TEM – transmission electron microscopy; TFA – total FA; TLC – thin-layer chromatography.

Introduction

Phosphorus (P) is a major nutrient central to functioning of the cell including the processes of energy and information storage and exchange. At the same time, P availability is limited and/or volatile in most of aquatic and terrestrial habitats [1-3]. Under such conditions, the ability to efficiently take up and store P against future shortage constitutes a key competitive advantage for microorganisms including microalgae. In the course of their evolution they acquired a set of sophisticated mechanisms collectively termed "luxury uptake" of nutrients, especially P [1, 2]. Luxury uptake of P in microalgae manifests itself particularly by taking up more P than is necessary to support their next cell cycle [4].

At the same time, P in form of inorganic orthophosphate, P_i cannot be stored in the cell in large amounts because of the risk of displacing metabolic reaction equilibria. This is indirectly confirmed by inhibitory effect of high concentrations of P_i on the growth of microalgal culture with obviously limited P storing capacity [5]. Likely, this is the reason of storing the bulk of P reserves in the cells, including the surplus P acquired during luxury uptake, in form of inorganic polyphosphate (PolyP). PolyP forms peculiar inclusions that were discovered in all types of cells including microalgal cells. The ubiquity of PolyP might be related with its hypothetical role in primordial template biosynthesis processes which are closely related with origin of life [6, 7]. Arguably, the main function of PolyP in the cell is P depot, although diverse roles are ascribed to these molecules such as storage of energy and facilitating of accumulation of physiologically important metal ions by counter-balancing their positive charges [8, 9].

Luxury nutrient uptake by microalgae, especially that of P, comes into spotlight increasingly often due to its high significance in nature and in human activities. The patterns of luxury uptake of P is an important determinant of population dynamics and productivity of phytoplankton and harmful algae blooms [10]. The kinetics and extent of luxury P uptake are central to rational design of wastewater biotreatment facilities based on cultivation of microalgae [11]. Another important reason is connected to the problem of sustainable consumption of P. Thus, increasing mining of rock phosphate (mainly for P fertilizers) and notoriously low (< 20%) efficiency of the mined P usage increases the anthropogenic P pollution of the environment, in addition to the threat of global P shortage [12, 13]. Sophisticated technologies were developed for P biocapture from waste streams e.g a widespread technique based on heterotroph bacteria—Enhanced Phosphorus Bioremoval, EPBR [14]. Alternative approaches for removal of P from wastewater with microalgae emerged featuring distinct advantages such as simultaneous removal of different nitrogen species, destruction of organic pollutants, suppression of pathogenic microflora, capture of the greenhouse gas CO_2 and NO_x as well as co-generation of P-enriched biomass suitable for conversion into slow-release P biofertilizer [15, 16].

A promising avenue for utilization of algal biomass enriched in P is its application as P biofertilizer [16]. Algal biomass was proposed as a vehicle to recover and recycle nutrients from manure and manure treatment effluents [15, 17]. The release of bioavailable P from inorganic forms via biomineralization [18] and mobilization of PolyP from the biomass has previously been reported. It is crucial that the release of P is slow enough for efficient absorption by crop plants reducing the probability of P wasting by washout typical of conventional mineral P fertilizers [19].

Even such a short consideration obviates the pivotal role of luxury P uptake in many nutrient-driven processes in natural ecosystems as well as in microalgae-based technologies for the nutrient recovery and recycling. At the same time reports on luxury P uptake are

surprisingly scarce whereas a wealth of literature exists on the mechanisms and regulation of P uptake under P-limiting conditions (for reviews, see e.g. [1, 2, 20]). Most of the previous reports on luxury P uptake described the phenomenology and biochemistry of P uptake and PolyP formation and consumption by different microalgae under diverse conditions, although the mechanistic understanding was and, in many aspects, is so far limited. In many cases, the published data were hardly comparable to each other since the growth conditions and the cultures were different (see e.g. [2, 9] and references therein).

Here, we report of recent advances in understanding of luxury P uptake phenomenon and underlying mechanisms. Emphasis in this work is on rapid changes taking place during transition from P starvation to ample P conditions, which are of special relevance to natural habitats with volatile P availability. Findings of this work are also important for the informed choice of P supply rate and the conditioning of microalgal culture necessary for the development of viable processes for generation of P-enriched microalgal biomass.

Methods

Microalgal strains and cultivation conditions

Since many seminal works in the field of P uptake and storage have been carried with *Chlorella* [5, 21-24], we employed the microalgal strains *Chlorella vulgaris* CCALA 256, *Parachlorella kessleri* CCALA 251 (obtained from the Culture Collection of Autotrophic Organisms, Institute of Botany—CCALA, Czech Acad. Sci., Třeboň) and *C. vulgaris* IPPAS C-1 (K.A. Timiryazev Institute of Plant Physiology—IPPAS, Russian Acad. Sci.) as the model systems in this work.

The pre-cultures grown in 0.75 L flasks in 0.3 L of BG-11 medium [25] at 40 μmol PAR photons $\cdot$ m^{-2} $\cdot$ s^{-1} and the atmospheric CO_2 level were kept at the exponential phase by daily dilution with the medium. At the beginning of each experiment, cells were harvested by centrifugation (1200 × *g* for 5 min), washed twice in fresh BG-11 medium, and resuspended in the same medium. For batch-cultivation experiments, the cultures were started at an initial chlorophyll (Chl) concentration and biomass content of 25 mg $\cdot$ L^{-1} and 0.4 g $\cdot$ L^{-1}, respectively.

In the lab-scale experiments the cells were grown in 1.5 L glass columns (6.6 cm internal diameter) in a temperature-controlled water bath at 27 °C and constant bubbling with air or 2.5% CO_2 : 80% air mixture prepared and delivered at a rate of 300 mL $\cdot$ min^{-1} (STP) using a PC-controlled gas mixer UFPGS-4 (Sovlab, Novosibirsk, Russia). Air passed through 0.22 μm bacterial filter (Merck-Millipore, Billerica, MA, USA) and pure (99.999%) CO_2 from cylinders were used. A continuous illumination of 480 μmol PAR photons $\cdot$ m^{-2} $\cdot$ s^{-1} by a white light-emitting diode source as measured with a LiCor 850 quantum sensor (LiCor, Lincoln NE, USA) in the center of an empty column was used. Culture pH was measured with a bench-top pH-meter (Hanna Instruments, Ann Arbor MI, USA).

In the experiments with cultivation in a V-bag bioreactor (NOVAgreen®), the cultures were initiated at 25 mg L^{-1} of chlorophyll (Chl) in 5 L of Tamiya medium [26] inside a greenhouse. The cultures were grown under combined illumination comprised by natural solar illumination and continuous illumination by fluorescent tubes (Sylvania T8 GroLux F18W/GRO, Belgium) at 250 μmol PAR quanta m^{-2} s^{-1} as measured at a bag surface with a LiCor 850 quantum sensor (LiCor, USA). The cultures were sparged with CO_2 : air (1 : 25, v/v) mixture at a

rate of 5 L min^{-1}. The culture growth was monitored via cell number, which was calculated using a haemocytometer or a Z2 Coulter counter (Beckman-Coulter, USA), and Chl content (see below).

To obtain the cultures with depleted internal P reserves, the cells were pelleted by centrifugation (5 min, 3000 *g*), washed with the corresponding P-free BG-11 or Tamiya medium, re-suspended in the same medium and incubated under the conditions described above in the P-free medium. The onset of P starvation was detected by a decline in the cell division rate. The cultures showing no significant increase in cell number for at least three consecutive days under our experimental conditions were considered as P-depleted and used for the further experiments.

Monitoring of growth and biomass accumulation

Growth of the cultures was monitored by measuring cell density of algal suspension using a Multisizer 3 particle analyzer (Beckman-Coulter, USA). Average growth rate, μ, was calculated as $\mu = [\log(N_{2)} - \log(N_1)]/(t_2 - t_1)$ where N_1 and N_2 are suspension cell densities at times t_1 and t_2, respectively.

Cell dry weight (DW) accumulation was determined gravimetrically based on cell dry weight (DW) measurements; Chl volumetric content was determined spectrophotometrically [27]. Briefly, an aliquot of the cell suspension was sampled from the PBR and the cells were harvested by centrifugation for 5 min at 3000 g. The cell pellet was washed with distilled water and used for DW determination. In routine measurements total Chl were extracted by heating the cell pellet for 5 min at 70 °C with 5 mL of with dimethyl sulfoxide (DMSO) per ca. 3.5 mg DW. The pigment concentrations were determined in the DMSO extracts with an Agilent Cary 300 spectrophotometer (Walnut Creek, CA, USA) using equations reported in [28].

All experiments were carried out in three biological replications, with two analytical replications for each of them. In figures, average values together with standard deviations are presented unless stated otherwise. The significance of differences was tested using ANOVA from the analysis toolpack of the Excel (Microsoft, USA) spreadsheet software.

Electron microscopy

The microalgae samples for transmission electron microscopy (TEM) were fixed in 2% (w/v) glutaraldehyde solution in 0.1 M sodium cacodylate buffer at room temperature for 0.5 h and then post-fixed for 4 h in 1% (w/v) OsO_4 in the same buffer. The samples, after dehydration through graded ethanol series including anhydrous ethanol saturated with uranylacetate, were embedded in araldite. Ultrathin sections were made with an LKB-8800 (LKB, Sweden) ultratome, stained with lead citrate according to Reynolds [29] and examined under JEM-1011 (JEOL, Tokyo, Japan) microscope.

The samples for nanoscale elemental analysis in TEM using energy-dispersive X-ray (EDX) spectroscopy were fixed, dehydrated and embedded in araldite as described above excepting the staining with uranylacetate and lead citrate. Semi-thin sections were made with a LKB-8800 (LKB, Sweden) ultratome and examined under JEM-2100 (JEOL, Japan) microscope equipped with a LaB_6 gun at the accelerating voltage 200 kV. Point (30 nm^2) EDX spectra were recorded using JEOL bright-field STEM module and X-Max X-ray detector system with ultrathin

window capable analyze light elements starting from boron (Oxford instruments, UK). The energy range of recorded spectra was 0-10 keV with a resolution of 10 eV per channel. This range includes biogenic elements (C, N, O, P, Ca, Mg, S, K, Na, Cl) peaks. Spectra were processed with INCA software (Oxford Instruments, UK) and presented in the range of 0.15–4 keV. At least 10 cells of every specimen were analyzed. Spectra were recorded from different parts of electron-dense inclusions (at least 35 measurements for every point) and from other (sub)compartments of microalgae cell (thylakoid membranes, pyrenoid, plastoglobuli, starch granules in chloroplast, mitochondrion, cytoplasmic oil bodies and nucleus).

Assay of phosphorus species in the medium and in the cells

The residual P_i and nitrate contents in the medium were checked daily with standard cuvette tests LCK 380 and LCK 350 (Hach Lange, Germany). The assessments of nitrate, orthophosphate and sulfate ion concentrations were also done using Thermo Dionex ICS 1600 HPLC (Sunnyvale, CA, USA) with a conductivity detector and IonPac AS12A (5µm; 2 × 250 mm) anionic analytical column with AG12A guard column (5µm; 2 × 50 mm). The column temperature was maintained at 30 °C. The ions were eluted isocratically with 2.7 mM sodium carbonate/0.3 mM sodium bicarbonate buffer (flow rate of 0.3 mL min^{-1}).

Total P in the lyophilized biomass samples were measured by ICP-MS (Element-2, Thermo Finnigan) at the Laboratory of Experimental Geochemistry of the Geological Faculty, Moscow State University [30]. Biomass samples were dissolved in 65% nitric acid (Suprapur®) and diluted by ultrapure EasyRure® deionized water. Indium was used as internal standard. The uncertainty of P concentration measurements ranged from 2% to 5% of the corresponding average depending on the sample mass.

To obtain information on P species, including polyphosphate, presence and distribution in the cell as well as its chemical surrounding, we employed in vivo ^{31}P NMR spectroscopy [31-33]. ^{31}P NMR spectra of dense (about 10^9 cells mL^{-1}) suspensions of the algae were recorded at 121.5 MHz at 25° C on an AMX300 wide-bore spectrometer (Bruker, Germany) equipped with a 20-mm ^{31}P probe. One-hour spectra were obtained by the accumulation of 7200 FID's in 1 h blocks with an accumulation time of 0.3 sec, a recycle time of 0.2 sec and by using a flip angle of 45°. The samples were prepared directly after harvest of the algal suspension by centrifugation and re-suspension in the P-free medium. 20 ml of the dense suspensions was transferred into the 20 mm NMR tube and directly measured after preparation. Methylene diphosphonic acid (0.2 M, pH 8.9), contained in an in situ capillary axially attached to the NMR tube, was used as a chemical shift marker having a chemical shift of 16.92 ppm relative to the chemical shift of 85% H_2PO_4 which is set at 0 ppm as general standard in ^{31}P NMR to scale the resonances of P-containing compounds [34]. Under these condition the g-ATP resonance in the spectra has a chemical shift value of –4.8 ppm [35] or –4.9 ppm [36] and NADH has a resonance position at –10.6 ppm. Both values are used in this paper as internal reference to calibrate the algal spectra.

Chlorophyll fluorescence measurements

The rapid Chl fluorescence transient (OJIP) and NPQ levels were recorded in a quartz cell (2 mm path length) with a Fluorpen FP100s PAM-fluorimeter (PSI, Drasov, Czech Republic) after 15 min dark adaptation according to the manufacturer's protocol. The chlorophyll fluorescence was

excited by a light-emitting diode (λ = 455 ± 5 nm) and detected in the range of 697–750 nm *(*[37, 38], see also Table S1).

Quantification of PolyP by Raman microscopy

For fast *in situ* quantification of PolyP within intact algal cells, a confocal Raman microscopy was used according to [39]. Briefly, a pellet of algal cells harvested by centrifugation was re-suspended in 1% w/v solution of low-gelling agarose (T = 39 °C), immediately spread as a single-cell layer between a quartz slide and coverslip and sealed with a CoverGrip sealant (Biotium, USA). The agarose immobilization was used to prevent movements of the cells during Raman mapping.

Two-dimensional Raman maps were acquired by a confocal Raman microscope WITec alpha300 RSA (WITec, Germany), laser excitation 532 nm (20 mW power at the focal plane) and an oil-immersion objective UPlanFLN 100×, NA 1.30 (Olympus, Japan). The spectral resolution of all Raman measurements was ca 6 cm^{-1}. The scanning step was 220 nm in both directions. Using an integration time of 0.1 s per cell voxel, Raman map of a typical *Chlorella* cell was acquired within ca 150 s. To remove the strong autofluorescence of chlorophyll, a wide-area, low-power photobleaching of the entire cell by a defocused 532-nm laser beam was applied prior to the mapping, according to [40]. Typically, 30–50 cells were measured for each specimen.

PolyP content in the cell was quantified as an integral Raman intensity of the prominent PolyP Raman band located at around 1160 cm^{-1}. Details of the data treatment and PolyP quantification were described recently in [39].

Lipidomic analysis

Total lipids were extracted from the microalgal cells as previously described [41]. Briefly, 100 mg of freeze-dried cells were heated at 75 °C in the presence of 500 µL DMSO for 10 min under continuous stirring; 5 mL methanol was then added, and extraction continued for 1 h at 4 °C under continuous mixing. DDW (5 mL) was added, followed by 10 mL of a hexane:diethyl ether mixture (1:2, v/v). Upon phase separation, the upper phase was collected, and the pH level of the bottom phase was adjusted to 3–4 by adding a few drops of 1 M HCl to facilitate extraction of acidic lipids. Extraction was repeated twice using a hexane:diethyl ether (1:1, v/v) mixture. All lipid fractions were collected and evaporated in a rotor vapor, transferred to a glass vial and stored under argon atmosphere in a small volume of chloroform. This method recovers over 85% of total fatty acids (TFA) compared to the direct transmethylation of dry biomass from *L. incisa* cells, which is impermeable to chloroform : methanol mixtures. All procedures were carried out in the presence of argon gas and under dimmed light to prevent oxidation of unsaturated lipids.

Total lipids were fractionated into neutral and polar lipids on silica cartridges (Bond Elute, Agilent, USA). Polar and neutral lipid classes were resolved by TLC as previously described [41]. To visualize the lipid spots, TLC plates were briefly sprayed with 8-anilino-1-naphthalene-sulfonic acid (0.05 % w/v in methanol) (Sigma, St. Louis, MO, USA) and observed under UV light. Individual lipid spots were scraped off the TLC plate, and the FA content and composition were determined as their methyl esters by GC-FID.

Fatty acid methyl esters (FAME) were obtained by direct transmethylation of freeze-dried biomass and isolated lipids in dry methanol containing 2% (v/v) H_2SO_4 at 80 °C for 1.5 h under argon atmosphere with continuous stirring. Heptadecanoic acid (C17:0) (Fluka, Buchs,

Switzerland) was added as an internal standard. The FAME were quantified on a Trace GC Ultra (Thermo, Milan, Italy) equipped with a flame ionization detector (FID) and programmed temperature vaporizing injector as previously described [27].

Studies of gene expression

In this work, we used sequencing of the whole transcriptome for discovery and selection of the genes potentially relevant to the phenomena observed during luxury uptake of P by the microalgal cells. The presence and the differential expression levels of these genes were further verified by RTPCR. Detailed description of the methods used in this part of the work could be found in Online Supplementary, brief description thereof is presented below.

For the transcriptome sequencing total RNA from the *C. vulgaris* IPPAS C-1 cells was isolated with RNeasy Kit (Qiagen, Germany) according to the manufacturer's protocol. For the real-time PCR, total RNA was isolated from the cells with RNeasy Plus Mini Kit (Qiagen, Germany) according to the protocol of the manufacturer (see also Supplementary Methods).

Prior to cDNA library construction, polyA-mRNA fraction was selected using oligo-dT magnetic beads (Illumina, San-Diego, CA, USA) and processed using NextFlex Rapid Directional RNA-Seq Kit (Bioo Scientific, Austin, TX, USA). cDNA libraries were quantified using Qubit 1.0 fluorometer (Invitrogen, Carlsbad, CA, USA) and quantitative PCR, diluted to 10 pM and sequenced using HiSeq2000 instrument from both ends of the fragment (read length = 100 nt) with TruSeq v.3 sequencing chemistry (Illumina, San-Diego, CA, USA). Raw data were processed with CASAVA v. 1.8.2. Assembly was performed using CLC genomics Workbench with following parameters: word size = 64, bubble size = 50, minimum contig length = 300.

The contigs were annotated by Blast2GO (www.blast2go.com) v3.0 InterPro [42] scan with Nr and Pfam annotation [43] in Gene Ontology (GO) database (http://geneontology.org/), and at Kyoto Encyclopedia of Genes and Genomes Pathway database (KEGG, http://www.genome.jp/kegg/) Automatic Annotation Server. Homologous sequences were searched against NCBI GeneBank (nucleotide collection nr/nt database) using BLAST (http://blast.ncbi.nlm.nih.gov/) [44]. Sequence data analysis, including multiple alignments, was conducted in Geneious v11 (www.biomatters.com).

Synthesis of the single-strand cDNA for real-time PCR (RT-PCR) was performed using QuantiTect Reverse Transcription Kit (Qiagen, Germany) according to the manufacturer's protocol. Primers were designed using the RealTime PCR Tool (Integrated DNA Technologies, Inc., https://eu.idtdna.com/scitools/Applications/RealTimePCR/) with the default parameters for the contigs putatively associated with the genes involved in the P_i transport, metabolism of polyphosphates, and the gene of endogenous control (see Table S2 and Figs. S3-S7).

Real-time PCR was performed using the QuantiTect SYBR Green PCR Kit (Qiagen, Germany) according to the manufacturer's recommendations, the QuantStudio 7 Flex Real-time PCR System (Thermo Fisher Scientific, USA) and the Applied Biosystems QuantStudio™ Real-time PCR Software Version 1.3 (Thermo Fisher Scientific, USA). All measurements were carried out with two biological and two analytical replicas. The expression of the target genes at different stages after re-feeding was calculated relatively to that recorded in the P-starved cells. The obtained data were processed using the Thermo Fisher Cloud Data Analysis software (Thermo Fisher Scientific, USA) with the default parameters.

Results and Discussion

Manifestations of P shortage and replenishment in culture growth and photosynthetic activity

As mentioned in the introduction, inconsistence of the data on luxury uptake of P in microalgae stems particularly from the using of microalgal cells which were not really P-starved. In other words, P reserves in these cell did not really drop to the minimum cell P quota (for a more detailed discussion on nutrient cell quotas, see [45]). Therefore, it become evident that the development of standardized experimental approach working across algal strains and cultivation systems is essential for the obtaining of consistent, reproducible, and comparable results.

We decided to employ microalgal cells with their cell P quota exhausted as much as possible (i.e. to a minimum cell P quota) under our experimental conditions and designated them as "P-starved" cells. Towards this end, the pre-cultures grown in the P-replete media were deprived of P and incubated under otherwise non-limiting conditions. For this kind of experiments, choice of a reliable marker of the onset of P starvation (exhaustion of the cell P quota) is important. It turned to be a non-trivial task since P shortage, as any important nutrient starvation, triggers multi-faceted responses including changes in cell lipid and pigment composition [46].

Eventually, cessation of cell division was chosen as the reliable manifestation of P starvation. After preliminary experiments, it became clear that depending on the specific experimental conditions employed, it takes a considerable time (normally, from five to ten days) to obtain the culture with cell P quota exhausted as completely as possible. The P deprivation of the cultures under our conditions was accompanied by a decline in Chl, increase of the Car/Chl ratio which was in line with the manifestations of P shortage recorded in other works (see [1] and references therein). Spectacular manifestations of the onset of P starvation were the decline in primary photochemistry quantum yield (Qy) and strong buildup of non-photochemical quenching of Chl fluorescence, NPQ (Fig. 1).

Microalgal cells grown in the absence of P limitation possess reserves of P, mostly in form of PolyP, sufficient to support several cell generations upon P deprivation [1, 2]. Indeed, a vigorous cell division continued for three days, after a one-day lag, upon the transfer of the cells to the P-free medium. Only by the fourth day of P starvation (in the bubble columns, see Methods) or several days later (in the Novagreen V-bags) the rate of cell division slowed down and resumed after P replenishment (Fig. 1A). Generally, the faster was cell division during the P deprivation of the culture, the sooner was observed the onset of P-starvation. This observation is in agreement with previous results that cell P reserves can be sufficient for a certain number of cell divisions (normally, 4−8 in *Chlorella*), but the time of the onset of P starvation also depends on other conditions (light and nitrogen availability, temperature, etc.). In addition, one should note that at this stage it is essential to determine the maximum time of P deprivation to obtain cells with depleted P reserves but still capable of fast recovery upon replenishment of P.

The cultures which did not show an increase in cell density for three days under our experimental conditions were accepted as "P-starved" initial cultures for the purpose of our experiments. Using the cultures conditioned in this way allowed obtaining reproducible results

in the subsequent experiments on luxury P uptake (re-feeding of the P-starved cells) described below regardless of the specific cultivation system and/or strain used in this work.

After establishing a standard protocol for obtaining of P-starved cells, we focused on luxury uptake of this nutrient after re-feeding of the P-starved cells with inorganic P (orthophosphate, P_i). The cell division resumed within one day after P replenishment (Fig. 1A). The cells also re-accumulated Chl after P re-feeding resulting in a decline of Car/Chl ratio (not shown). The rate of the recovery of the pigment composition after P re-feeding was commensurate to that of cell division recovery.

The primary photochemistry of the microalgal cells was more sensitive to P availability than photosynthetic pigment composition or cell division rate. Thus, a drop of the Qy and corresponding increase in NPQ occurred before the decline in Chl and cell division slowdown (Fig. 1B). Accordingly, Qy and NPQ recovered after P re-feeding faster than the piment composition and cell division rate (Fig. 1A).

The depletion of the phosphometabolite pool and PolyP in the cell was confirmed by *in vivo* ^{31}P-NMR spectroscopy (Fig. 2). The peak attributable to inorganic phosphate (P_i) still present in the spectra of the cells of all three organisms, its amplitude was the highest in *C. vulgaris* CCALA 256. At the same time, the partitioning of the intracellular P_i between major cellular compartments (cytoplasm, chloroplast and vacuole) cannot be determined from the NMR spectra of the P-depleted algal cell, which contained a single symmetrical P_i resonance. This also indicated that the pH of these compartments was nearly the same [31], suggesting that a low degree of membrane energization under the P starvation conditions. Only in the cells of *C. vulgaris* IPPAS C-1 a noticeable level of sugar-phosphates was revealed in addition to P_i probably indicative of relatively more active metabolism in this alga even under P starvation conditions. At the same time, all the spectra lacked the signatures of energy-rich molecules e.g. ADP and ATP, spectral details attributable to polyphosphate were also absent suggesting the overall metabolic quiescence of the P-starving cells.

Luxury P uptake induces specific rearrangements of the cell lipidome

One of the major depots of P in the microalgal cells is constituted by phospholipids—important components of cell membrane lipids. On the one hand, P starvation and recovery from it induce considerable rearrangements of the cell membranous structures and lipid reserves (Fig. 3; [47, 48]). On the other hand, nutrient deprivation is often employed in microalgal biotechnology for induction of lipid accumulation in the cells. As was revealed by TEM, P shortage induces accumulation of lipid droplets, LD (Fig. 3) and a reduction of chloroplast together with its membrane apparatus (thylakoid system). After re-feeding of the cells, the LD disappear, and the chloroplast is recovered together with its thylakoid membranes. These processes occurred along with the re-start of cell division.

The changes in lipid content and composition documented during P starvation and after P re-feeding in our experiments reflected the acclimation to P shortage and, afterwards, to ample P availability (Fig. 4). The most spectacular changes were recorded in the abundance of neutral reserve lipid, TAG (Fig. 3). It corresponded to the observed dynamics of the LD formation which increased in the P-starving cells and declined after their re-feeding with P_i. Such dynamics of TAG is characteristic of nutrient limitation of microalgal cells and their

recovery from it [49]. During this process, TAG, as well as starch, accommodates photofixed carbon which cannot be consumed by anabolic reactions under the stress thereby alleviating the risk of photooxidative damage to the cell [49, 50].

The onset of P starvation was manifested by characteristic changes in cell glycolipids represented by the two major classes: non-bilayer-forming monogalactosyldiacylglycerols, MGDG and bilayer-forming digalactosyldiacylglycerols, DGDG. These lipids enriched with polyunsaturated FA are the major constituents of the chloroplast thylakoids membranes [51]. Their ratio plays an important role in the adjustment of thylakoid membrane biophysical properties under stress, so an increase in the ratio of DGDG/MGDG is a generic pattern of stress acclimation of photosynthetic cells [52, 53]. P starvation under our experimental conditions also lead to a decline in DGDG/MGDG ratio (Fig. 4).

We also recorded peculiar rearrangements in the lipidome of P-sarving cells typical of stress, such as an increase in sulfolipids (sulfoquinovosildiacylglycerol, SQDG). At the same time, we did not observe a relatively widespread manifestation of P shortage—increase in betain lipids (represented in the studied species by diacylglyceryltrimethylhomoserine, DGTS; Fig. 4).

The P-containing lipid classes did not show a consistent pattern of changes in our experiments. Thus, we did not observe a sizeable decline of the phospholipid classes during P starvation although there was a sizeable increase in phosphatydilcholine (PC) proportion after re-feeding of the P-starved cells (Fig. 4). The apparent lack of the P starvation response in P-lipids of the studied microalgae at first glance might seem counter-intuitive. At the same time, it is in line with vast diversity of lipidome-related response to P-limitation documented in microalgae, some of them might be not so straightforward [47, 48]. A plausible explanation of relative stability of P-lipid content under the P shortage conditions might involve their essential role in maintaining of the cell membrane homeostasis so these lipids were retained even under harsh P deficiency. Interestingly, DGTS often serving as the substitute of P-lipids in P-starving cells, did not show a considerable increase in our experiments (Fig. 4) suggesting a different mechanism of cell membrane stabilization under P shortage conditions. Clearly, further research is needed to reveal a generic pattern of lipidome response in microalgae on the background of volatile P availability.

Relationship between cell division and P_i uptake rates after re-feeding of P-starved cells

Survey of the available literature (see e.g. [1, 2] and references therein) suggested that microalgal cultures with different P nutrition prehistory differ dramatically in terms of their P_i uptake potential. At the same time, consistent data on P uptake kinetics are hard to come by in the literature, although remarkable exceptions exist [22]. Here, we tried to systematically study the P_i uptake and formation of PolyP in the P-starved cultures of standardized *Chlorella* cultures with cell P quota exhausted to the minimum (see above).

The P-starved cells re-fed with P_i exhibited a polyphasic kinetics of P_i uptake (Fig. 5). Two phases were clearly distinguished: the first, fast phase of P_i uptake took place within first 1–2 h from the moment of re-feeding and the second phase, which was characterized by slower P_i uptake. In the studied microalgae, this phase started 2–4 h later and roughly corresponded to

the period of the exponential cell division in the re-fed culture (Fig. 5). It is also possible to distinguish the third phase (slow-down of P_i uptake along with slow-down of cell division for the reasons other than P deficiency, e.g. self-shading).

During the first (fast) phase the cells of all studied microalgae took up P_i at a high (6–9 ng d^{-1} $cell^{-1}$) rate. However, cell division did not resume at this stage hence no correlation between P_i uptake and cell division rate was recorded (Fig. 5) but the influx of P_i into the cell correlated with its external concentration (Fig. S1). This P_i uptake pattern resembled that described in microalgae as 'overshoot' or overcompensation [2] exhibited by P-limited cells transferred to a P-replete environment [22].

The vigorous uptake of P_i at this phase resulting in a temporary rise of P content, calculated on elemental P, in the biomass up to 5–6% of DW (Fig. 6). This is not far from 10% DW achieved in a heterotroph bacterium *Acinetobacter* [54] used in the enhanced biological phosphorus removal (EBPR) processes [14]. A rough calculation of a global potential of such non-optimized P-uptake capacity of algae leads to an estimate that approximately 7 000 km^2 of algae production area (less than, e.g. area of Cyprus) would be required to sequester 7 Mt of phosphorus that is world-wide annually lost from animal manure [13]. This calculation assumes a realistic growth rate of algae (30–40 g DW · m^{-2} · day^{-1}; [55] and 7% P in dry weight observed during the period of peak P_i uptake under our experimental conditions. With P uptake by algae that would be enhanced by an optimization, the required area would be further correspondingly decreased.

Although the intracellular P content in the actively dividing cells was modest (< 2% DW) in comparison with that detected during the overshoot following the P refeeding, its metabolic turnover is immense [56]. In this case a considerable part of P_i entering the cell is converted to nucleoside phosphates and sugar phosphates and is consumed for biosynthesis of nucleic acids, mainly DNA and ribosomal RNA which are the most abundant of the nucleic acid molecules in the cell [56], and phospholipids. Obviously, this was the case under our experimental conditions: judging from the ^{31}P NMR data, the exponentially growing cells featured diverse pools of phosphometabolites such as nucleoside phosphates and sugar phosphates (Fig. 2). In particular, P_i and sugar-phosphate levels were likely higher than in the P_i-depleted cells except *C. vulgaris* CCALA 256. Relatively low amount of polyphosphate was discovered in the exponential culture cells of *C. vulgaris* CCALA 256 and *P. kessleri* CCALA 251. The spectrum of *C. vulgaris* IPPAS C-1 lacked a detectable signal of polyphosphate but showed on the contrary the three resonances of ATP (Fig. 2). The lack of the NMR spectral signature of P storage (sub)compartments such as vacuolar P_i pool or PolyP in the case of *C. vulgaris* IPPAS C-1 can be explained by its high growth rate of which was the fastest among the studied microalgae. Therefore, most of the absorbed P_i was likely involved in the cell metabolism so there hardly can be excess P_i routed to storage compartments. This suggestion was indirectly confirmed by the relatively high pH of the P_i-containing compartments as could be deduced from the NMR spectra and the presence of all three ATP resonances [31, 36].

One should also remember that even the rapidly dividing cells, as well as those at terminal stages of P starvation, still can retain some PolyP, likely belonging to low-mobile (acid-insoluble) fraction [23, 57]. This PolyP fraction is hardly distinguishable on ^{31}P NMR spectra, but it is clearly visible on TEM images (see e.g. Fig. 3c). One can speculate that this fraction of PolyP characterized likely by a low availability for the cell metabolism contributes, together with the essential nucleic acids, P-lipids and other organic P fractions, to the minimum or subsistence P quota of the microalgal cell.

Notably, uptake of P_i from the medium at a very high rate was observed only for a limited time (normally, 60 min in our experiments). Within one day after replenishment of P_i in the medium, all the studied microalgae resumed exponential growth. After the first 24 h of cultivation in the P-replete medium, the P_i uptake rate declined approximately by an order of magnitude in comparison with the "peak" uptake rate; it exhibited a close ($r^2 > 0.8$) relationship with the culture growth rate throughout the rest of the observation period (Fig. 5). These relationships followed a similar pattern: P_i uptake rate was proportional to μ values below 0.2 (characteristic of the initial period of the culture recovery from P starvation; observed 1–1.5 d after re-feeding) and the onset of stationary phase (days 5–9 after re-feeding, see Fig. 2). In the range of higher μ values (0.2–0.9) typical of the mid-exponential phase (days 1.5–4 after re-feeding) the relationship 'μ vs. P_i uptake rate' tended to saturate (Fig. 5).

After three days of cultivation in the P-replete medium, the growth rate of the cultures started to slow down manifesting the onset of stationary phase, a simultaneous decline in the rate of P_i uptake from the medium took place during this period. After the 6th day of the cultivation under the P-replete condition, the cultures reached the early stationary phase; only a marginal decline in P_i was recorded during the last six days of the experiment (Fig. 5).

Notably, a different pattern of subcellular P pools was revealed by the ^{31}P NMR spectra of the cells from the stationary-phase cultures in comparison to that documented in the exponential cultures grown in the P-replete medium (Fig. 2c). Thus, the peak attributable to PolyP was much more pronounced in the ^{31}P NMR spectra of all these cells; the highest amplitude of this peak was detected in *C. vulgaris* CCALA 256 and the lowest in *C. vulgaris* IPPAS C-1.

In the cells of the cultures at early stationary phase, distinguishable P_i pools were revealed in the chloroplast and cytoplasm (featuring the same pH value) of *C. vulgaris* CCALA 256 (2.21 ppm, pH = 6.8) and *P. kessleri* CCALA 251 (2.25 ppm, pH = 6.9) whereas a smaller pool was associated with the vacuole (1.59 ppm, pH 6.4 in both cases). The ^{31}P NMR spectrum of *C. vulgaris* IPPAS C-1 showed only a trace vacuolar P_i (1.59 ppm, pH 6.4) next to the main P_i resonance at 2.37 ppm (pH 6.9). The levels of sugar-phosphates were similar in all studied microalgae. As the cells from the exponential-phase culture, the cells of stationary-phase culture of *C. vulgaris* IPPAS C-1 possessed a relatively high level of P-metabolites involved in energy exchange e.g. ATP/ADP (with an ATP/ADP ratio > 1) suggesting a more vigorous metabolism. This finding, as well as the lowest level of mobile polyphosphate and vacuolar P_i, are in good agreement with the highest growth rate of *C. vulgaris* IPPAS C-1. The highest amount of mobile PolyP and vacuolar P_i was found in *C. vulgaris* CCALA 256, the strain which demonstrated the lowest growth rate. Accordingly, this strain had a lower ATP/ADP ratio indicative of low overall metabolic activity. The levels of P-metabolites and PolyP in *P. kessleri* CCALA 251 were close to that found in *C. vulgaris* CCALA 256 as well as the ATP/ADP ratio > 1.

As a result of steady uptake of P_i at a moderately high rate (Fig. 5), the biomass content of P was as high as 2 % of cell DW (Fig. 6) whereas a typical gravimetric share of P in dry weight of natural phytoplankton at ca. 0.9 %, corresponding to <1% estimate of [58]. The P biomass content recorded in the present work roughly corresponded to the current estimations for the microalgae gown in P-rich environment. Thus, values as high as 1.8 % DW were found in the microalgal cells fed by swine manure [59]; levels up to 4% were reported for the cultures frown in wastewater [60].

Overall, the kinetics of P_i absorption and the levels of intracellular P accumulation in our experiments are evident of operation of the 'luxury uptake' mechanism originally described in

[61]. An important feature of luxury P uptake is that it takes place even in P-sufficient culture i.e. without a prior exposure of the cells to P starvation [62]. The luxury P uptake has probably evolved as an adaptation of microalgae to volatile P availability or as a competitive strategy aimed at starving the competitor [63].

Relationship of the PolyP formation, P_i uptake, and cell division kinetics

It is commonly accepted that PolyP is normally accumulated in microalgal cell when P is ample in the medium; the PolyP reserves are metabolized during periods of P shortage [22, 39, 64]. There are several fractions of PolyP differing in their function in the cell, stability, and dependence on light energy for their synthesis [23]. Indeed, under our experimental conditions the P-starved cells which ceased to divide contained no PolyP detectable by NMR (Fig. 2) although small P-containing inclusions were found on TEM images (see above).

The transient very high P content (> 4–5% DW, Fig. 6) recorded in these cells after their re-feeding with P_i drew our attention to possible involvement of PolyP in storing at least part of the P taken up in large excess shortly after their re-feeding. Most of the techniques mentioned above turned to be unsuitable for this task due to insufficient time resolution: thus, acquisition of a reliable NMR spectrum requires least several hours. In principle, it was possible to use an enzymatic PolyP assay, but this procedure is laborious and expensive. Eventually, we accepted a recently developed approach based on confocal Raman microscopy calibrated vs. analytical PolyP assay yielding data on PolyP distribution with subcellular resolution (for detailed description, see [39]).

Using Raman microscopy as a rapid method of PolyP screening in individual cells, we followed the kinetics of the PolyP content after re-feeding, along with the culture growth (Fig. 7). The PolyP content in the cells increased and peaked approximately within 4–10 h after re-feeding of the P-starved culture with P_i. This transient peak of PolyP roughly corresponded to the fast phase of P_i uptake from the medium and the period when the cells exhibited the highest percentage of P in their DW. Notably, the extent of PolyP accumulation depended on the concentration of the external P_i added during re-feeding S2. The PolyP level in the cell declined rapidly when the cell division resumed after recovery from P starvation (Fig. 7). Interestingly, a similar transient rise of PolyP can be seen in Fig. 3 in the paper by Aitchison and Butt [22] suggesting a transient storing of P_i until the end of the lag phase and culture recovery. Even more pronounced transient peak of PolyP was observed in *Parachlorella kessleri* NIES-2152 [46]. Collectively, the findings mentioned above suggest that PolyP content is peaking when the maximum P*i* influx coincides with a slow cell division rate.

The cell PolyP content in the exponentially growing culture remained low. It started to increase again when cell division slowed down reaching early stationary phase on the background of ample P_i in the medium (Fig. 2). At the same time, it was not as high as during the lag phase recorded shortly upon re-feeding (Fig. 6). Generally, the upward trend of PolyP is in line with that recorded in stationary cultures of *Chlorella* in P-sufficient media [1, 22].

Taking into account the dynamics of cell PolyP content, culture growth and P_i uptake, one can generalize that the rate of PolyP formation in the microalgal cells is directly related with the P_i influx in the cell and inversely related with cell division rate. In turn, the P_i influx depends on the external P_i concentration and the extent of the cell acclimation to P deficiency. In particular, the acclimation to scarce P conditions manifests itself as the expression of high-

affinity P_i transporters, which will be elaborated on below, see also [20]. The enhanced biosynthesis of PolyP upon slowdown of cell division can be explained in terms of channeling of the P_i absorbed in excess during luxury uptake and did not consumed in biosynthesis of cell structural components to storage in form of PolyP, the most abundant P reserve in microalgal cell [65].

Polyphosphates in microalgal cell possess a peculiar ultrastructural organization

Taking into account possible presence of different PolyP fractions (mobile or acid-soluble and acid-insoluble, the latter is not readily visible in the NMR spectra) combination of ultrastructural studies (analytical TEM) and ^{31}P NMR spectroscopy is expected to provide a more comprehensive picture of PolyP within microalgal cell. To obtain a further insight into subcellular distribution of polyP, we employed an analytical electron microscopy technique known as energy dispersive X-ray analysis (EDX) which has been applied previously to analyze P in the electron-dense inclusions in the cells of chlorophytes [66, 67].

The cells of the studied microalgae sampled at stationary growth phase contained numerous electron-dense inclusions in their vacuoles (Fig. 8a); these inclusions were scarce the P-starving or exponentially growing cells (Fig. 8d). Analysis of the point EDX spectra taken from the inclusions showed that the elemental compositions of these structures were dominated by P and oxygen, divalent metals (Mg and Ca) were also present but monovalent metal ions such as K, were missing (Fig. 8c, f, i), most likely because of chemical fixation used for the sample preparation for EDX. Since the P-containing inclusions were highly osmiophylic, the peaks of P partially overlapped with those of Os (Fig. 8c, i). Nevertheless, the resolution of the EDX measurements was sufficient for reliable determination of P in the samples. The characteristic EDX peak of P was also detected in nuclei (not shown) but its amplitude was considerably lower than in the spectra from the P-containing inclusions. The point EDX spectra from other structures (sub)compartments of the microalgal cell (thylakoid membranes, pyrenoid, plastoglobuli, starch granules in chloroplast, cytoplasmic oil bodies) lacked the peak attributable to P (not shown).

Collectively, the ^{31}P NMR- and EDX-based evidence suggests that the electron-dense inclusions observed in the cells of stationary phase cultures are indeed PolyP granules [68]. A closer look at the P-containing inclusions identified as PolyP granules in the cells of *C. vulgaris* C-1 *и C. vulgaris* 256 on the conventional and analytical TEM micrographs revealed the regions with highly ordered structure. The latter were most pronounced in *C. vulgaris* 256 cells sampled at the stationary growth phase after re-feeding with P_i (Fig. 9). The structured PolyP granules were frequently in close contact with tonoplast membrane from the inside.

In certain regions of the PolyP grain cross-sections electron-dense filaments were revealed interleaved with low electron density spacers, both 4.90 ± 0.12 nm wide (Fig. 9a). These structures resembled a multi-wire cable pattern documented in our previous work [69]. At higher magnifications (Fig. 9b), the filaments were apparent as electron-dense granules forming chains or zigzag patterns. These granules were assembled in packs interspersed with low electron-density matter and interconnected with 1.64 ± 0.07 nm wide bridge-like structures of moderate electron density. On the cross-cut of PolyP granules these structures formed cellular clusters resembling a cross-cut multiwire cable (Figs. 9b, 10). In the “cross-cut” pattern, the electron-dense particles were 5.07 ± 0.31 nm in size interconnected with several bridge-like structures, each of them was 1.31 ± 0.07 nm wide. One can interpret these TEM micrographs as images of

longitudinally- and cross-cut sections of long packs of electron-dense grain chains embedded in an electron-transparent matter, twisted within the vacuole lumen (Fig. 10). Interestingly, a similar ultrastructural pattern was demonstrated revealed in the vacuolar PolyP granules of another chlorophytes (Table S4). In view of the aforementioned findings, we assumed that processes of the PolyP chains biosynthesis and their transportation into the vacuolar lumen are coupled in the cells of the studied microalgae. Mechanistically, these processes might be similar to those taking place in acidocalcisomes of yeast cells with the participation of a large membrane-bound complex historically named VTC (vacuolar transporter chaperone) but representing essentially a multienzyme machine for PolyP biosynthesis [70-73].

The group of Ota [46] who studied P-containing inclusions in the chorophyte *Parachlorella kessleri* NIES-2152 showed that the organic matter forming the bridge-like sealing caps incorporated into these inclusions is nether sugar nor lipid. It is also known that the PolyP chains can form complexes with poly-(R)-3-hydroxybutirate (PHB) [74]. Such complexes were revealed in the membranes of many organisms (seep. 46 in [9]) although the fine structure of these complexes remains unelucidated). In view of these findings, the bridge-like PolyP chain-sealing structures within the PolyP vacuolar inclusions are most likely constituted PHB. The ultrastructural organization of the P-rich vacuolar inclusions in the studied microalgae we hypothesized that that many PolyP chains are synthesized simultaneously by multienzyme VTC-like complexes producing PolyP and PHB grouped together to form raft-like structures in the tonoplast (Fig. 10).

Generally, presence of an ordered ultrastructural organization in a cell structure often suggests participation of complex molecular machine in its biogenesis. One of the examples can be the carotenoid crystals with ordered structure [75]. In an analogy with this, we hypothesize that the formation of PolyP granules, at least in the microalgal cell vacuole, is not a stochastic process carried e.g. by a relatively simple enzyme freely floating in the vacuolar lumen. On the contrary, a more complex molecular machine associated with the vacuolar membrane (tonoplast) is expected to be involved in the process of PolyP biosynthesis and the formation of P-containing inclusions in the vacuoles. With this in mind, we focused on the analysis of *C. vulgaris* transcriptome in search of possible candidate genes encoding parts of this molecular machines. We also looked for other genes potentially involved in the implementation of the observed kinetics of P_i uptake and PolyP accumulation in this alga.

Insights into molecular mechanisms potentially involved in luxury P uptake and storage

As a further stage of the work, we screened the transcriptome of *Chlorella vulgaris* IPPAS C-1 for the genes differentially expressed under the experimental conditions used in this work (P-starvation with subsequent P re-feeding). We expected to discover genes involved in P_i transport into the cell and/or storing it in form of PolyP. In view of the kinetics of P_i uptake and PolyP accumulation revealed in this work, we choose more frequent sampling during first several hours including also characteristic stages of the culture development such as logarithmic and early exponential. The annotated transcriptome was than searched by relevant keywords. The search results were filtered for the significance level (FDR < 0.05) and minimum differential expression threshold ($\log_2$FC > 2). As a result, a subset of transcripts of the genes with contrasting expression patterns (table S3) was selected including one encoding VTC-like protein (GenBank ID MK334249), one H^+/P_i symporter (GenBank ID MK334251) and Na^+/P_i symporter (GenBank ID MK334252) as well as a purple acid phosphatase (GenBank ID MK334253) (table S3). These genes were used as targets for subsequent RTPCR analysis of differential expression level.

Induction and repression of polyphosphate polymerases

During the analysis of the *C. vulgaris* IPPAS C1 transcriptome we found the homologs of subunits of VTC (GenBank ID: MK334249, Fig. S8), the polyphosphate polymerase assembling the PolyP chains. The auto-translated amino-acid sequence of the annotated transcript MK334249 possessed a high identity with Vtc1, Vtc2 and Vtc4 proteins of green microalgae and fungi including yeast (Figs. 11, S4). Due to the high identity level, it was not possible to assign the transcript sequence to Vtc1, Vtc2 or Vtc4 with confidence. Still, all these proteins belong to the Poly-P synthesizing VTC complex [70] so its expression level can be a proxy of VTC activity under our experimental conditions. To verify the differential expression of the putative VTC component, we employed RT-PCR using the target region of the transcript which displayed 84% identity to Vtc1 protein of a closely related species *C. variabilis*.

To test the possible involvement of this gene in metabolism of PolyP during P starvation and re-feeding under our experimental conditions we compared the expression level of the other selected candidate genes during P-starvation and subsequent re-feeding of the *C. vulgaris* IPPAS C1 culture. Following the accepted practices [76], we selected a gene encoding a putative plant and algal ubiquitinase E3 homolog (GenBank ID: MK334250, 98% identity with ubiquitinase E3 of *C. sorokiniana*) as the reference basing on a high and stable expression level of its expression under our experimental conditions.

The results of RTPCR essentially confirmed the preliminary assessment carried out with RNASeq. Both approaches showed that the changes in the kinetics of P_i uptake rate and PolyP accumulation recorded in our experiments were accompanied by distinct changes in the expression level of the genes putatively involved in P_i uptake and PolyP metabolism. Thus, within 120 min after re-feeding of P-starving cells with Pi the expression of the gene encoding the VTC-like protein (transcript MK334249) and the Na^+/P_i-symporter (transcript MK334251) increased 3.8 and 3.3 times respectively. On the contrary, the expression levels of the H^+/P_i symporter (GenBank ID MK334252) and purple acid phosphatase (transcript GenBank ID MK334253) declined 10.5 and 20 times respectively (Fig. 12).

At the exponential phase (3 d after re-feeding), the expression level of the gene encoding the VTC-like protein returned to the level of the P-starving cells but at the stationary phase (7–9 d after re-feeding) increased again (47 times as compared to that of the starving cells). The expression pattern of the gene encoding the VTC-like protein was largely in agreement with the observed kinetics of PolyP in the cells documented by NMR (Fig. 2) and other independent methods (Figs. 7). In particular, the transient VTC up-regulation roughly corresponded to the transient peak of PolyP formation in the cell, particularly in vacuoles; the second rise of the expression of the gene putatively encoding this protein also corresponded to the increase in PolyP at the stationary growth phase (Fig. 12).

These findings further support the involvement of the VTC-like protein in the biosynthesis of the PolyP in green microalgae. At the same time, this mechanism of PolyP biosynthesis might not be ubiquitous. Thus, the genome of a red microalga *Cyanidioschyzon merolae* apparently lacks homologs of the Vtc4-type of PolyP polymerase [77] but contains a homolog of the prokaryotic PolyP kinase gene *ppk1* [78]. Yagisawa, Kuroiwa, Fujiwara and Kuroiwa [77] hypothesized that a PPK1, a PolyP-kinase, homolog is responsible for the formation of the PolyP in *C. merolae* cells during first hours after re-feeding of P-starving cells. The authors of this work also suggested an alternative, VTC-independent mechanism of PolyP biosynthesis. According to

their hypothesis, the synthesis of PolyP begins in cytosol or in small vacuoles, then the small PolyP granules are exported to larger vacuole(s) where they are accumulated and/or enlarged. However, the latter mechanism is still questionable in view of the reported toxicity of short-chain PolyP in yeast cells [70, 73]. On the other hand, the hypothetical transportation of nascent PolyP into the vacuole can manifest a mechanism of coping with the potential toxicity of the short-chain PolyP in microalgal cell.

To the best of our knowledge, this is the first work elucidating the differential expression of VTC-like homologs as a function of P availability in green microalgae. At the same time, there were reports on the modulation of VTC expression during P starvation of a coccolitophore *Emiliania huxleyi* [79] and a diatom *Thalassiosira pseudonana* [80]. Interestingly, both of the microalgal species showed a considerably higher expression of *vtc* genes in the cells grown in the P-depleted medium than in those incubated in a P-replete medium. Unexpectedly, PolyP content of *T. pseudonana* cells was higher during P shortage in the medium than during cultivation on a P-replete medium [80]. The authors relate these phenomena, which might seem counterintuitive, by the natural acclimation of the studied organisms to volatile P availability in the marine aquatic habitats. Under such conditions, the ability to efficiently sequester P_i and store it as PolyP in the cell might be crucial for successful competition with other microorganisms [81].

Difficulties with studies of the expression of genes encoding the enzymes involved in PolyP biosynthesis are related to reversibility of the reactions catalyzed by them, this is also true for vtc4 PolyP-polymerase (see p. 157 in [81]). On the one hand, it means that the up-regulation of vtc4 might evidence both PolyP accumulation and mobilization. On the other hand, the up-regulation of vtc4 and similar enzymes and PolyP decline are not mutually exclusive events. Importantly, in many works the cells are sampled in the beginning of the P-shortage induced slow-down of cell division. Strictly speaking, these cells might not be really P-starved since the culture growth did not stopped completely. In our experiments with P re-feeding we used the cell with exhausted PolyP cell depot and down-regulated genes of the VTC-like proteins, so the experiments described here do not likely suffer from this limitation.

Changeover of P_i transporters after re-feeding of the P-starved cells

Since the metabolism of PolyP depends, among other factors, on the influx of P_i into the cell [22], genes of the putative extracellular phosphatase releasing P_i from organic compounds and two types of putative P_i transporters were included into the analysis of differential gene expression (Figs. S5 and S6). Specifically, we selected the putative transcript MK334251, which was highly identical to a conservative domain of high-affinity Pi transporters and Na^+/P_i-symporters of microalgae (Fig. S5). Another target was MK334252, a putative transcript highly similar to H^+/P_i symporters in microalgae (Fig. S6). The RTPCR primers were designed using a cv11978 region 91% similar to a P_i transporter and a MK334251 region 89% identical to a H^+/P_i symporter of *C. sorokiniana*. In addition to this, MK334253, a putative transcript resembling a purple acid phosphatase from microalgae (Fig. S7). Corresponding RTPCR primers were designed using a MK334253 region 92% identical to a purple acid phosphatase from *C. sorokiniana*.

The very high rate of P_i absorption observed during the first phase of P-starving microalgal cells' re-feeding (Fig. 5) is believed to result from the activity of high-affinity P_i-uptake system ensuring efficient pumping of P_i into the cell when its concentration is low [1, 2, 20]. This is compatible with previous findings of the P_i uptake peak in the cells in which cell

division has been arrested [22] so the P_i entering the cell is not spent e.g. for the synthesis of new cell building blocks. The high-affinity P_i uptake system is functioning under low-P conditions and complete P starvation because the corresponding high-affinity P_i transporter proteins are expressed and present in the cell membrane under limiting P_i levels. The high-affinity P_i transporters rapidly pump P_i into the cell but are saturated quickly by the incoming P_i. After re-feeding of the P-starved cells, the high-affinity P_i transporter expression is rapidly down-regulated and replaced by low-affinity P_i transporters which are normally expressed when P_i is ample in the medium [20].

In our experiments, the two studied genes of P_i transporters were downregulated in the in the P re-fed cells than in P-starved cells (Fig. 12). Such a behavior is typical of high-affinity Pi transporters which are up-regulated during P shortage in the medium and down regulated when P is ample [82-84]. Furthermore, the studied putative Na^+/P_i symporter of *C. vulgaris* IPPAS C-1 displayed a high identity to high-affinity P_i-transporters earlier annotated in *C. variabilis*, *Tetraselmis chuii* and *Ectocarpus siliculosus* genomes (Fig. SS5).

Our results remind inverted gene expression patterns recorded e.g. in a model microalga *C. reinhardtii* during P-starvation. Thus, P starvation induces down-regulation of the high-affinity P_i transporters PTB2 [82-84] and PTA3 [84]. Different patterns of P_i transporter gene expression were recorded during the first several hours after P re-feeding of the P-starved cells. Thus, the expression of the putative Na^+/P_i symporter is induced upon the re-feeding of the P-starved cells whereas that of the putative H^+/P_i symporter was repressed (Fig. 12). Taking into account these expression patterns, it is possible to assign the putative H^+/P_i symporter to high-affinity P_i transporters with a high specificity to P_i but relatively low uptake rate [82-84].

After re-feeding the P-starving cells end up in the medium with ample P where the low-affinity P_i transporters are more efficient due to their higher uptake rate in comparison with high-affinity P_i transporters [85]. This hypothesis also helps to explain the rapid repression of the putative H^+/P_i symporter (10.5 time decline within 2 h after re-feeding). On the contrary, the putative Na^+/P_i symporter is likely a high-affinity P_i transporter judging from its rapid up-regulation upon re-feeding of the P-starved cells. Our data showed that a high level of the expression of the high-affinity P_i transporter can be retained for a certain time after P re-feeding which is not typical for this type of P_i transporters [84, 86]. It is therefore conceivable that the putative Na^+/P_i symporter, a high-affinity transporter studied in our work, can contribute to the rapid P_i uptake observed shortly after re-feeding of the P-starved cells due to its relatively slow down-regulation.

Other P acquisition mechanisms

The putative acid purple phosphatase (APF) was down-regulated under ample P conditions (during exponential and stationary growth phases) in comparison with the P-starved cells (1.5 and 1.9 times lower, respectively), although the repression was most pronounced within first hours after re-feeding (Fig. 12). This expression pattern is compatible with the known function of APF in higher plants [87, 88]: these enzymes are excreted to release bioavailable P_i from P-containing organic matter. Re-feeding with the excess of P_i removes the need to obtain P_i from the extracellular organics so the expression of the putative APF declines. During the exponential and stationary growth phase the concentration of the available P_i in the medium declines due to uptake by the microalgal cells leading to a moderate up-regulation of the APF relatively to the level recorded within first hours after re-feeding.

Generally, the recorded expression pattern of the putative APF in *C. vulgaris* IPPAS C-1 resembles the mirrored trend of APF expression in P-starving organisms: it increases under P starvation and declines under ample P conditions. Remarkably, these changes are very rapid in in *C. vulgaris* IPPAS C-1: the expression of APF in this microalga declines 20 times within 2 h upon their re-feeding.

Implications for biotechnology

Understanding the mechanisms and patterns of luxury P uptake and PolyP metabolism is crucial for solving real-world P biosequestration problems. In particular, luxury nutrient, especially P uptake, is central to operation of wastewater stabilization ponds and wastewater treatment plants but currently these processes are limited to "a black box understanding of the bulk population" [89].

Application of the microalgae biomass grown in wastewater to field crops as a biofertilizer is a promising way of its utilization [16, 19]. In contrast to P-rich bacterial biomass from EBPR process [90], P-rich algal biomass acts as a slow-release P fertilizer [91] due to a slow decomposition of PolyP by the soil microbial phosphatases [19]. Accordingly, enrichment of the algal biomass with PolyP is an important quality parameter of microalgal biomass-derived P biofertilizer. Our findings showed that the highest PolyP content is achieved shortly after re-feeding of P-starved microalgae with P_i. At the same time, this is a transient PolyP buildup: soon after resumption of cell division PolyP content started to decline, therefore timely harvesting the PolyP-rich biomass is crucial for the biofertilizer applications.

Since the P-starved cells express the features of high-affinity P_i uptake, they represent the most suitable culture type for final treatment of wastewater (so called "polishing" stage). Larger amounts of biomass but only moderately enriched with PolyP can be obtained by harvesting stationary-phase cells grown in ample P-media. Rapidly dividing cells of exponentially growing P-sufficient cultures displayed a moderate but sustained rate of P_i uptake. Biomass generated at this stage is rich in bioantioxidant pigments (carotenoids) and proteins so it is potentially suitable as a feed additive.

Concluding remarks

In this work, we focused on luxury phosphorus uptake in microalgae, the process important from both fundamental and practical standpoints but remaining vastly underexplored. We re-approached this phenomenon using recently developed advanced techniques (analytical TEM, scanning micro-Raman spectroscopy, transcriptome and PCR analysis) which were not available at the time when the seminal works on the luxury P uptake were carried out. As a result, a deeper mechanistic insight into luxury uptake and intracellular storing of P was gained.

A significant hassle for studies of P uptake in microalgae was constituted by disparate experimental conditions yielding hardly comparable results. We employed a standardized "feast–famine" protocol based on the using of pre-starved microalgal cells with exhausted cell P quota. It turned to be a crucial step for obtaining reproducible results comparable across diverse cultivation systems, different microalgal strains and even species.

Both luxury Pi uptake and its intracellular storage in form of PolyP exhibited a peculiar kinetics which was related with cell division rate. The first, fast phase of exogenic P_i uptake (< 4

h upon re-feeding of the P-starved cells) is likely determined by high-affinity P_i transporters. Although these transporters saturate quickly, it is likely that they are ample in the membrane of P-starving cell. Within this short period, a very high P content (> 6% DW) can be reached. This finding is of direct relevance for biological removal of P from waste streams with microalgae with subsequent utilization of the resulting biomass as environmental-friendly biofertilizer.

Since at that time cell division does not yet resume and the demand of P for the anabolic process in the cell is low, the P taken up in a large excess is transiently stored in the form of PolyP, mostly in the cell vacuole. Judging from ordered ultrastructural organization of vacuolar PolyP granules and characteristic expression pattern of a gene encoding a VTC-like protein, the rapid turnover of PolyP is most likely associated with operation of a VTC-like multienzyme complex of tonoplast.

Soon after P_i re-feeding, the high affinity P uptake system is replaced by the low-affinity uptake system, the cell division resumes by that time. Exponential division of microalgal cells is characterized by a much slower P_i uptake at a rate related to actual cell division rate and a low PolyP content. At this stage, the cell is expected to spend most of the acquired P for building components of new cells, so there is little, if any, surplus P available for storage. Accordingly, the VTC-like complex is down-regulated. It is up-regulated only at the onset of stationary phase due to light limitation on the background of ample P_i in the medium, when a second peak of PolyP accumulation is detected.

Overall, the results of this work show that luxury uptake of P is a complex phenomenon manifesting concerted operation of diverse mechanisms ensuring efficient uptake of P*i*, balancing the influx of P_i against the current metabolic sink capacity, storing the surplus P_i in form of PolyP and its remobilization on demand. We believe that the key finding of this study will help to better understand the nutrient availability-driven changes in microalgal communities in natural ecosystems and artificial cultivation systems. They will also facilitate the creation of engineered strains for biotechnological application for efficient usage of P in agriculture and wastewater treatment. A deep mechanistic understanding of luxury P uptake is at the basis of rational design of efficient bioprocesses for sustainable P usage so there is a clear need of a systematic study of luxury P uptake in different algal strains under a wide range of relevant environmental, biological and treatment conditions.

Acknowledgements

The authors are grateful to Dr. Olga Baulina for her invaluable help with electron microscopy, to Mrs. Isabel Meuser. Mr. Andres Sadowsky, and Mr. Pavel Scherbakov for their dedicated technical help and Dr. Andrey Bychkov for his help with ICP-MS assays.

Funding

Financial support of BioSC is greatly appreciated. The ultrastructure studies were carried out at the User Facilities Center of M.V. Lomonosov Moscow State University and funded by Russian Foundation for Basic Research [grant # 18-29-25050]. Photosynthetic activity was analyzed with support of RFBR [grant # 19-04-00509]. Partial support of the «RUDN University Program 5-100» is gratefully acknowledged.

Author contributions

AS conceived and designed the experiments, analyzed the results and carried out the photosynthetic activity measurements. IS and LS carried out the lab-scale cultivation experiments. IKG performed the lipidomics analysis and treated the data. AL and SV measured photosynthetic activity. IM and IZ performed the RNASeq experiments and treated the data. TI performed the analytical TEM measurements and DGE assessment. OG supervised TEM imaging, carried out the conventional TEM and morphometry. EV and OK supervised the rtPCR experiments and treated the data. PM carried out the Raman measurements and treated the data. CD and MV measured and interpreted the NMR spectra. IK supervised the chlorophyll fluorescence measurements. LN conceived the P-depletion experiments and supervised the large-scale cultivation experiments. All authors wrote and approved the final version of the manuscript.

References

[1] A. Cembella, N. Antia, P. Haerrison, G.-Y. Rhee, The Utilization of Inorganic and Organic Phosphorous Compounds as Nutrients by Eukaryotic Microalgae: A Multidisciplinary Perspective: Part 2, Critical Reviews in Microbiology, 11 (1984) 13-81.

[2] A.D. Cembella, N.J. Antia, P.J. Harrison, The utilization of inorganic and organic phosphorous compounds as nutrients by eukaryotic microalgae: A multidisciplinary perspective: Part I, Critical reviews in microbiology, 10 (1982) 317-391.

[3] S. Haneklaus, H. Bloem, E. Schnug, Hungry Plants—A Short Treatise on How to Feed Crops under Stress, Agriculture, 8 (2018).

[4] G.-Y. Rhee, A continuous culture study of phosphate uptake, growth rate and polyphosphate in *Scenedesmus* sp., Journal of Phycology, 9 (1973) 495-506.

[5] Q. Li, L. Fu, Y. Wang, D. Zhou, B.E. Rittmann, Excessive phosphorus caused inhibition and cell damage during heterotrophic growth of Chlorella regularis, Bioresour Technol, 268 (2018) 266-270.

[6] L. Achbergerová, J. Nahálka, Polyphosphate-an ancient energy source and active metabolic regulator, Microb Cell Fact, 10 (2011) 14170-14175.

[7] M.J. Gray, W.Y. Wholey, N.O. Wagner, C.M. Cremers, A. Mueller-Schickert, N.T. Hock, A.G. Krieger, E.M. Smith, R.A. Bender, J.C. Bardwell, U. Jakob, Polyphosphate is a primordial chaperone, Molecular cell, 53 (2014) 689-699.

[8] I.S. Kulaev, V.M. Vagabov, Polyphosphate metabolism in micro-organisms, Advances in microbial physiology, Elsevier1983, pp. 83-171.

[9] I. Kulaev, I. Vagabov, T. Kulakovskaya, The Biochemistry of Inorganic Polyphosphates, 2 ed., John Wiley & Sons, Ltd, Chichester, England, 2004.

[10] L. Aubriot, S. Bonilla, Rapid regulation of phosphate uptake in freshwater cyanobacterial blooms, Aquatic Microbial Ecology, 67 (2012) 251-263.

[11] N. Brown, A. Shilton, Luxury uptake of phosphorus by microalgae in waste stabilisation ponds: current understanding and future direction, Reviews in Environmental Science and Bio/Technology, 13 (2014) 321-328.

[12] D. Cordell, S. White, Life's Bottleneck: Implications of Global Phosphorus Scarcity and Pathways for a Sustainable Food System, Annual Review of Environment and Resources, 39 (2014).

[13] V. Smil, Phosphorus in the environment: natural flows and human interferences, Annual review of energy and the environment, 25 (2000) 53-88.

[14] T. Mino, M. van Loosdrecht, J. Heijnen, Microbiology and biochemistry of the enhanced biological phosphate removal process, Water Research, 32 (1998) 3193–3207.

[15] W. Mulbry, E.K. Westhead, C. Pizarro, L. Sikora, Recycling of manure nutrients: use of algal biomass from dairy manure treatment as a slow release fertilizer, Bioresource Technology, 96 (2005) 451-458.

[16] A. Solovchenko, A.M. Verschoor, N.D. Jablonowski, L. Nedbal, Phosphorus from wastewater to crops: An alternative path involving microalgae, Biotechnology advances, 34 (2016) 550–564.

[17] A.C. Wilkie, W.W. Mulbry, Recovery of dairy manure nutrients by benthic freshwater algae, Bioresource Technology, 84 (2002) 81-91.
[18] G. Zhao, J. Du, Y. Jia, Y. Lv, G. Han, X. Tian, The importance of bacteria in promoting algal growth in eutrophic lakes with limited available phosphorus, Ecological Engineering, 42 (2012) 107-111.
[19] K. Ray, C. Mukherjee, A.N. Ghosh, A way to curb phosphorus toxicity in the environment: use of polyphosphate reservoir of cyanobacteria and microalga as a safe alternative phosphorus biofertilizer for Indian agriculture, Environmental science & technology, 47 (2013) 11378-11379.
[20] A.R. Grossman, M. Aksoy, Algae in a phosphorus-limited landscape, in: W. Plaxton, H. Lambers (Eds.) Annual Plant Reviews, Phosphorus Metabolism in Plants, Wiley-Blackwell2015, pp. 337-374.
[21] C. Schreiber, H. Schiedung, L. Harrison, C. Briese, B. Ackermann, J. Kant, S.D. Schrey, D. Hofmann, D. Singh, O. Ebenhöh, W. Amelung, U. Schurr, T. Mettler-Altmann, G. Huber, N.D. Jablonowski, L. Nedbal, Evaluating potential of green alga Chlorella vulgaris to accumulate phosphorus and to fertilize nutrient-poor soil substrates for crop plants, Journal of Applied Phycology, (2018).
[22] P. Aitchison, V. Butt, The relation between the synthesis of inorganic polyphosphate and phosphate uptake by Chlorella vulgaris, Journal of Experimental Botany, 24 (1973) 497-510.
[23] S. Miyachi, R. Kanai, S. Mihara, S. Miyachi, S. Aoki, Metabolic roles of inorganic polyphosphates in *Chlorella* cells, Biochimica et Biophysica Acta, 93 (1964) 625-634.
[24] S. Miyachi, S. Miyachi, Modes of formation of phosphate compounds and their turnover in Chlorella cells during the process of life cycle as studied by the technique of synchronous culture, Plant and Cell Physiology, 2 (1961) 415-424.
[25] R. Stanier, R. Kunisawa, M. Mandel, G. Cohen-Bazire, Purification and properties of unicellular blue-green algae (order Chroococcales), Microbiology and Molecular Biology Reviews, 35 (1971) 171-205.
[26] H. Tamiya, Mass Culture of Algae, Annual review of plant physiology, 8 (1957) 309-334.
[27] D. Pal, I. Khozin-Goldberg, Z. Cohen, S. Boussiba, The effect of light, salinity, and nitrogen availability on lipid production by *Nannochloropsis* sp., Applied microbiology and biotechnology, 90 (2011) 1429-1441.
[28] A. Solovchenko, M. Merzlyak, I. Khozin-Goldberg, Z. Cohen, S. Boussiba, Coordinated carotenoid and lipid syntheses induced in *Parietochloris incisa* (Chlorophyta, Trebouxiophyceae) mutant deficient in Δ5 desaturase by nitrogen starvation and high light, Journal of Phycology, 46 (2010) 763-772.
[29] E. Reynolds, The use of lead citrate at high pH as an electron-opaque stain in electron microscopy, The Journal of Cell Biology, 17 (1963) 208.
[30] Y.A. Popova, A.Y. Bychkov, S. Matveeva, Behavior of lanthanides during the formation of the Svetloe deposit, Chukotka, Geochemistry International, 54 (2016) 732-738.
[31] M. Ginzburg, R. Ratcliffe, T. Southon, Phosphorus metabolism and intracellular pH in the halotolerant alga *Dunaliella parva* studied by ^{31}P-NMR, Biochimica et Biophysica Acta (BBA)-Molecular Cell Research, 969 (1988) 225-235.
[32] J.-B. Martin, R. Bligny, F. Rebeille, R. Douce, J.-J. Leguay, Y. Mathieu, J. Guern, A ^{31}P Nuclear magnetic resonance study of intracellular pH of plant cells cultivated in liquid medium, Plant Physiology, 70 (1982) 1156-1161.
[33] F. Mitsumori, O. Ito, Phosphorus-31 nuclear magnetic resonance studies of photosynthesizing *Chlorella*, FEBS Letters, 174 (1984) 248-252.
[34] S. Hesse, G. Ruijter, C. Dijkema, J. Visser, Measurement of intracellular (compartmental) pH by ^{31}P NMR in *Aspergillus niger*, Journal of Biotechnology, 77 (2000) 5-15.
[35] J. Sianoudis, A. Küsel, T. Naujokat, W. Offermann, A. Mayer, L. Grimme, D. Leibfritz, Respirational activity of *Chlorella fusca* monitored by in vivo P-31 NMR, European Biophysics Journal, 13 (1985) 89-97.
[36] S.J. Hesse, G.J. Ruijter, C. Dijkema, J. Visser, Intracellular pH homeostasis in the filamentous fungus Aspergillus niger, European Journal of Biochemistry, 269 (2002) 3485-3494.
[37] K. Maxwell, G. Johnson, Chlorophyll fluorescence-a practical guide, Journal of Experimental Botany, 51 (2000) 659-668.
[38] A. Solovchenko, O. Solovchenko, I. Khozin-Goldberg, S. Didi-Cohen, D. Pal, Z. Cohen, S. Boussiba, Probing the effects of high-light stress on pigment and lipid metabolism in nitrogen-starving microalgae by measuring chlorophyll fluorescence transients: Studies with a Δ5 desaturase mutant of *Parietochloris incisa* (Chlorophyta, Trebouxiophyceae), Algal Research, 2 (2013) 175-182.

[39] S.a.r. Moudříková, A. Sadowsky, S. Metzger, L. Nedbal, T. Mettler-Altmann, P. Mojzes, Quantification of Polyphosphate in Microalgae by Raman Microscopy and by a Reference Enzymatic Assay, Analytical Chemistry, 89 (2017) 12006-12013.
[40] Š. Moudříková, P. Mojzeš, V. Zachleder, C. Pfaff, D. Behrendt, L. Nedbal, Raman and fluorescence microscopy sensing energy-transducing and energy-storing structures in microalgae, Algal Research, 16 (2016) 224-232.
[41] I. Khozin-Goldberg, S. Didi-Cohen, I. Shayakhmetova, Z. Cohen, Biosynthesis of eicosapentaenoic acid (EPA) in the freshwater eustigmatophyte Monodus subterraneus (Eustigmatophyceae), J Phycol, 38 (2002) 745-756.
[42] P. Jones, D. Binns, H.-Y. Chang, M. Fraser, W. Li, C. McAnulla, H. McWilliam, J. Maslen, A. Mitchell, G. Nuka, InterProScan 5: genome-scale protein function classification, Bioinformatics, 30 (2014) 1236-1240.
[43] S. Götz, J.M. García-Gómez, J. Terol, T.D. Williams, S.H. Nagaraj, M.J. Nueda, M. Robles, M. Talón, J. Dopazo, A. Conesa, High-throughput functional annotation and data mining with the Blast2GO suite, Nucleic Acids Research, 36 (2008) 3420-3435.
[44] S.F. Altschul, W. Gish, W. Miller, E.W. Myers, D.J. Lipman, Basic local alignment search tool, Journal of Molecular Biology, 215 (1990) 403-410.
[45] M. Pahlow, A. Oschlies, Optimal allocation backs Droop's cell-quota model, Marine Ecology Progress Series, 473 (2013) 1-5.
[46] S. Ota, M. Yoshihara, T. Yamazaki, T. Takeshita, A. Hirata, M. Konomi, K. Oshima, M. Hattori, K. Bisova, V. Zachleder, S. Kawano, Deciphering the relationship among phosphate dynamics, electron-dense body and lipid accumulation in the green alga Parachlorella kessleri, Sci Rep, 6 (2016) 25731.
[47] J.P. Canavate, I. Armada, I. Hachero-Cruzado, Interspecific variability in phosphorus-induced lipid remodelling among marine eukaryotic phytoplankton, New Phytol, (2016).
[48] J.P. Canavate, I. Armada, I. Hachero-Cruzado, Aspects of phosphorus physiology associated with phosphate-induced polar lipid remodelling in marine microalgae, J Plant Physiol, 214 (2017) 28-38.
[49] M. Vítová, K. Bišová, S. Kawano, V. Zachleder, Accumulation of energy reserves in algae: From cell cycles to biotechnological applications, Biotechnology Advances, 33 (2015) 1204-1218.
[50] A. Solovchenko, Physiological role of neutral lipid accumulation in eukaryotic microalgae under stresses, Russian Journal of Plant Physiology, 59 (2012) 167-176.
[51] I. Khozin-Goldberg, U. Iskandarov, Z. Cohen, LC-PUFA from photosynthetic microalgae: occurrence, biosynthesis, and prospects in biotechnology, Applied microbiology and biotechnology, (2011) 1-11.
[52] B. Zorin, D. Pal-Nath, A. Lukyanov, S. Smolskaya, S. Kolusheva, S. Didi-Cohen, S. Boussiba, Z. Cohen, I. Khozin-Goldberg, A. Solovchenko, Arachidonic acid is important for efficient use of light by the microalga Lobosphaera incisa under chilling stress, Biochimica et Biophysica Acta (BBA) - Molecular and Cell Biology of Lipids, 1862 (2017) 853-868.
[53] G. Garab, B. Ughy, R. Goss, Role of MGDG and non-bilayer lipid phases in the structure and dynamics of chloroplast thylakoid membranes, Lipids in Plant and Algae Development, Springer2016, pp. 127-157.
[54] J.W. van Groenestijn, G.J. Vlekke, D.M. Anink, M.H. Deinema, A.J. Zehnder, Role of cations in accumulation and release of phosphate by Acinetobacter strain 210A, Applied and environmental microbiology, 54 (1988) 2894-2901.
[55] J. Doucha, K. Lívanský, High Density Outdoor Microalgal Culture, in: R. Bajpai, A. Prokop, M. Zappi (Eds.) Algal Biorefineries, Springer Netherlands2014, pp. 147-173.
[56] L.M. Blank, The cell and P: from cellular function to biotechnological application, Current Opinion in Biotechnology, 23 (2012) 846-851.
[57] S. Miyachi, H. Tamiya, Distribution and turnover of phosphate compounds in growing *Chlorella* cells, Plant and Cell Physiology, 2 (1961) 405-414.
[58] J.U. Grobbelaar, Algal nutrition:mineral nutrition, in: A. Richmond (Ed.) Handbook of Microalgal Culture: Biotechnology and Applied Phycology

Blackwell Publishing, Oxford, UK, 2004, pp. 97–115.

[59] E. Kebede-Westhead, C. Pizarro, W.W. Mulbry, Treatment of swine manure effluent using freshwater algae: Production, nutrient recovery, and elemental composition of algal biomass at four effluent loading rates, Journal of Applied Phycology, 18 (2006) 41-46.
[60] N. Powell, A. Shilton, S. Pratt, Y. Chisti, Luxury uptake of phosphorus by microalgae in full-scale waste stabilisation ponds, Water Science & Technology, 63 (2011) 704-709.
[61] B.H. Ketchum, The absorption of phosphate and nitrate by illuminated cultures of Nitzschia closterium, American Journal of Botany, (1939) 399-407.
[62] S. Eixler, U. Karsten, U. Selig, Phosphorus storage in *Chlorella vulgaris* (Trebouxiophyceae, Chlorophyta) cells and its dependence on phosphate supply, 45 (2006) 51-60.
[63] C. de Mazancourt, M.W. Schwartz, Starve a competitor: evolution of luxury consumption as a competitive strategy, Theoretical Ecology, 5 (2012) 37-49.
[64] T. Albi, A. Serrano, Inorganic polyphosphate in the microbial world. Emerging roles for a multifaceted biopolymer, World J Microbiol Biotechnol, 32 (2016) 27.
[65] A. Kuhl, Phosphorus, in: W. Stewart (Ed.) Algal Physiology and Biochemistry, Blackwell Scientific, Oxford, 1974, pp. 636–654.
[66] J. Voříšek, V. Zachleder, Redistribution of phosphate deposits in the alga *Scenedesmus quadricauda* deprived of exogenous phosphate—an ultra-cytochemical study, Protoplasma, 119 (1984) 168-177.
[67] J. Adamec, J.H. Peverly, M.V. Parthasarathy, Potassium in polyphosphate bodies of *Chlorella pyrenoidosa* (Chlorophyceae) as determined by x-ray microanalysis, Journal of Phycology, 15 (1979) 466-468.
[68] M. Siderius, A. Musgrave, H. Ende, H. Koerten, P. Cambier, P. Meer, CHLAMYDOMONAS EUGAMETOS (CHLOROPHYTA) STORES PHOSPHATE IN POLYPHOSPHATE BODIES TOGETHER WITH CALCIUM1, Journal of phycology, 32 (1996) 402-409.
[69] A. Shebanova, T. Ismagulova, A. Solovchenko, O. Baulina, E. Lobakova, A. Ivanova, A. Moiseenko, K. Shaitan, V. Polshakov, L. Nedbal, Versatility of the green microalga cell vacuole function as revealed by analytical transmission electron microscopy, Protoplasma, 254 (2017) 1323–1340.
[70] R. Gerasimaite, S. Sharma, Y. Desfougeres, A. Schmidt, A. Mayer, Coupled synthesis and translocation restrains polyphosphate to acidocalcisome-like vacuoles and prevents its toxicity, J Cell Sci, 127 (2014) 5093-5104.
[71] M. Hothorn, H. Neumann, E.D. Lenherr, M. Wehner, V. Rybin, P.O. Hassa, A. Uttenweiler, M. Reinhardt, A. Schmidt, J.J.S. Seiler, Catalytic core of a membrane-associated eukaryotic polyphosphate polymerase, Science, 324 (2009) 513-516.
[72] O. Müller, M.J. Bayer, C. Peters, J.S. Andersen, M. Mann, A.J.T.E.J. Mayer, The Vtc proteins in vacuole fusion: coupling NSF activity to V0 trans-complex formation, 21 (2002) 259-269.
[73] R. Gerasimaitė, A. Mayer, Enzymes of yeast polyphosphate metabolism: structure, enzymology and biological roles, Biochemical Society Transactions, 44 (2016) 234-239.
[74] R. Reusch, Transmembrane ion transport by polyphosphate/poly-(R)-3-hydroxybutyrate complexes, BIOCHEMISTRY C/C OF BIOKHIMIIA, 65 (2000) 280-295.
[75] A. Kaczor, K. Turnau, M. Baranska, In situ Raman imaging of astaxanthin in a single microalgal cell, Analyst, 136 (2011) 1109-1112.
[76] H. Alexander, B.D. Jenkins, T.A. Rynearson, M.A. Saito, M.L. Mercier, S.T.J.F.i.m. Dyhrman, Identifying reference genes with stable expression from high throughput sequence data, 3 (2012) 385.
[77] F. Yagisawa, H. Kuroiwa, T. Fujiwara, T. Kuroiwa, Intracellular Structure of the Unicellular Red Alga Cyanidioschyzon merolae in Response to Phosphate Depletion and Resupplementation, Cytologia, 81 (2016) 341-347.
[78] M.P. Whitehead, P. Hooley, M.R. Brown, Horizontal transfer of bacterial polyphosphate kinases to eukaryotes: implications for the ice age and land colonisation, BMC research notes, 6 (2013) 221.
[79] S.T. Dyhrman, S.T. Haley, S.R. Birkeland, L.L. Wurch, M.J. Cipriano, A.G.J.A. McArthur, E. Microbiology, Long serial analysis of gene expression for gene discovery and transcriptome profiling in the widespread marine coccolithophore Emiliania huxleyi, 72 (2006) 252-260.
[80] S.T. Dyhrman, B.D. Jenkins, T.A. Rynearson, M.A. Saito, M.L. Mercier, H. Alexander, L.P. Whitney, A. Drzewianowski, V.V. Bulygin, E.M.J.P.o. Bertrand, The transcriptome and proteome of the diatom Thalassiosira pseudonana reveal a diverse phosphorus stress response, 7 (2012) e33768.

[81] S.T. Dyhrman, Nutrients and their acquisition: phosphorus physiology in microalgae, The physiology of microalgae, Springer2016, pp. 155-183.
[82] I. Kobayashi, S. Fujiwara, K. Shimogawara, T. Kaise, H. Usuda, M.J.P. Tsuzuki, c. physiology, Insertional mutagenesis in a homologue of a Pi transporter gene confers arsenate resistance on Chlamydomonas, 44 (2003) 597-606.
[83] C.-W. Chang, J.L. Moseley, D. Wykoff, A.R.J.P.p. Grossman, The LPB1 gene is important for acclimation of Chlamydomonas reinhardtii to phosphorus and sulfur deprivation, 138 (2005) 319-329.
[84] J.L. Moseley, C.-W. Chang, A.R.J.E.c. Grossman, Genome-based approaches to understanding phosphorus deprivation responses and PSR1 control in Chlamydomonas reinhardtii, 5 (2006) 26-44.
[85] A. Grossman, H. Takahashi, Macronutrient utilization by photosynthetic eukaryotes and the fabric of interactions, Annual review of plant biology, 52 (2001) 163-210.
[86] F.D. Pitt, S. Mazard, L. Humphreys, D.J. Scanlan, Functional characterization of Synechocystis sp. strain PCC 6803 pst1 and pst2 gene clusters reveals a novel strategy for phosphate uptake in a freshwater cyanobacterium, Journal of bacteriology, 192 (2010) 3512-3523.
[87] G.G. Bozzo, E.L. Dunn, W.C.J.P. Plaxton, cell, environment, Differential synthesis of phosphate-starvation inducible purple acid phosphatase isozymes in tomato (Lycopersicon esculentum) suspension cells and seedlings, 29 (2006) 303-313.
[88] J.C. Del Pozo, I. Allona, V. Rubio, A. Leyva, A. De La Peña, C. Aragoncillo, J.J.T.P.J. Paz-Ares, A type 5 acid phosphatase gene from Arabidopsis thaliana is induced by phosphate starvation and by some other types of phosphate mobilising/oxidative stress conditions, 19 (1999) 579-589.
[89] N. Brown, A. Shilton, Luxury uptake of phosphorus by microalgae in waste stabilisation ponds: current understanding and future direction, Reviews in Environmental Science and Bio/Technology, 13 (2014) 321-328.
[90] L.E. de-Bashan, Y. Bashan, Recent advances in removing phosphorus from wastewater and its future use as fertilizer (1997–2003), Water Research, 38 (2004) 4222-4246.
[91] N. Powell, A. Shilton, S. Pratt, Y. Chisti, Phosphate release from waste stabilisation pond sludge: significance and fate of polyphosphate, Water Science and Technology, 63 (2011) 1689.
[92] R. Strasser, M. Tsimilli-Michael, A. Srivastava, Analysis of the chlorophyll *a* fluorescence transient, in: *G. Papageorgiou*, *Govindjee* (Eds.) Chlorophyll a fluorescence: a signature of photosynthesis, Springer2004, pp. 321–362.
[93] N. Guex, M.C. Peitsch, SWISS-MODEL and the Swiss-Pdb Viewer: an environment for comparative protein modeling, Electrophoresis, 18 (1997) 2714-2723.
[94] M. Remmert, A. Biegert, A. Hauser, J. Söding, HHblits: lightning-fast iterative protein sequence searching by HMM-HMM alignment, Nature Methods, 9 (2012) 173-175.
[95] A. Rzhetsky, M. Nei, A simple method for estimating and testing minimum-evolution trees, Molecular Biology and Evolution, 9 (1992) 945.
[96] R.C. Edgar, MUSCLE: multiple sequence alignment with high accuracy and high throughput, Nucleic Acids Research, 32 (2004) 1792-1797.
[97] M. Larkin, G. Blackshields, N. Brown, R. Chenna, P.A. McGettigan, H. McWilliam, F. Valentin, I.M. Wallace, A. Wilm, R. Lopez, Clustal W and Clustal X version 2.0, Bioinformatics, 23 (2007) 2947-2948.
[98] J. Felsenstein, Confidence limits on phylogenies: an approach using the bootstrap, Evolution, 39 (1985) 783-791.

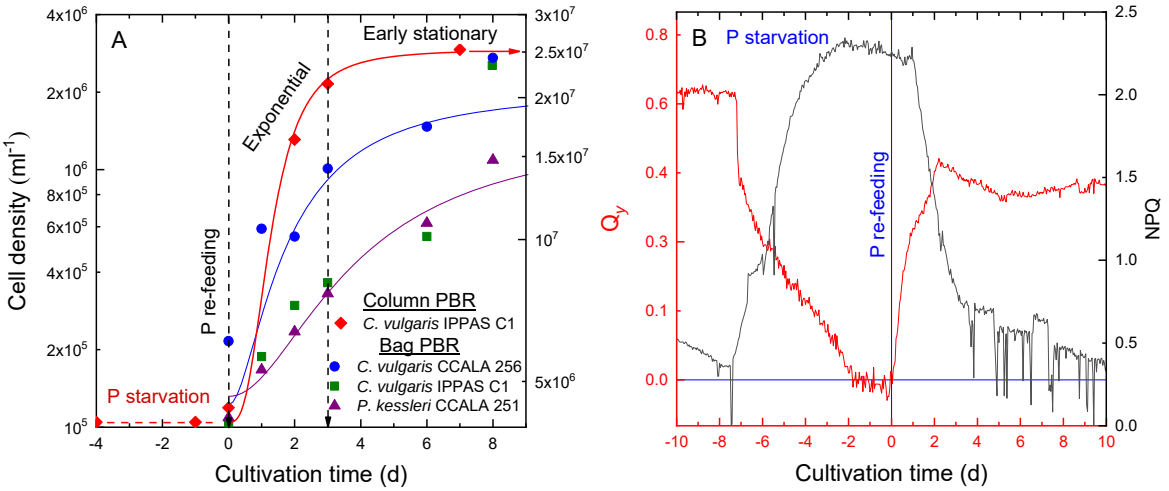

Fig. 1. Growth and photosynthetic activity of the studied microalgae during re-feeding of pre-starved culture with P_i. (A) Growth of the P-starved cultures of *Parachlorella kessleri* CCALA 251, *C. vulgaris* IPPAS C1, and *C. vulgaris* CCALA 256 after replenishment of P in the medium. (B) Effects of P starvation and subsequent P re-feeding on non-photochemical quenching of chlorophyll fluorescence in *Chlorella vulgaris* CCALA 256.

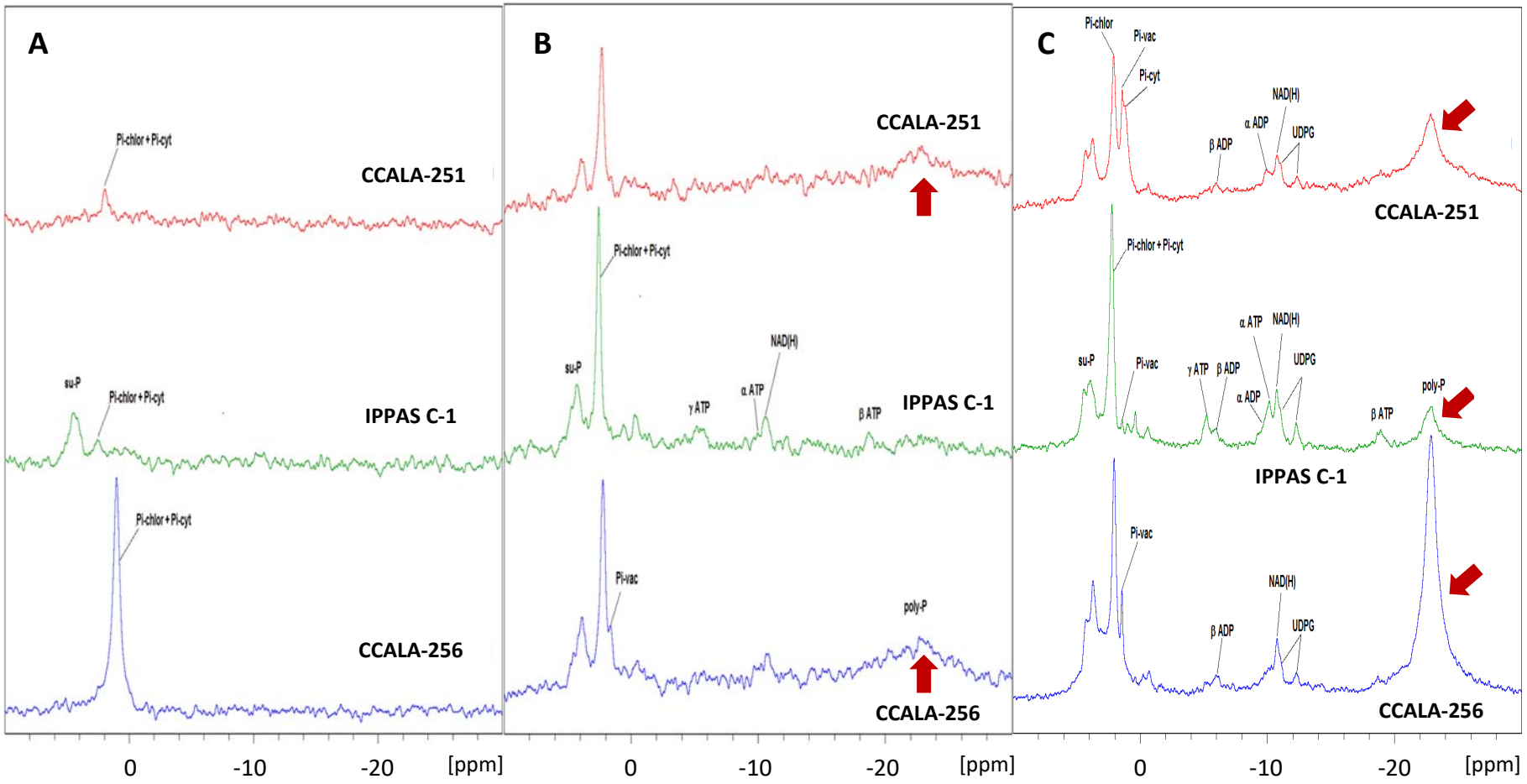

Fig. 2. ^{31}P-NMR spectra of dense suspensions of (top to bottom) *C. vulgaris* CCALA 256, *C. vulgaris* IPPAS C1, and *P. kessleri* CCALA 251 recorded (A) after eight days of P starvation, (B) after three days upon P_i replenishment in the medium (exponential growth phase), and (C) at the early stationary growth phase. P_i-chlor—the Pi pool in the chloroplast; P_i-vac—the P_i pool in the vacuole; P_i-cyt—the P_i pool in the cytoplasm; su-P—sugar-phosphates; poly-P—polyphosphate (corresponding peak is marked by arrow).

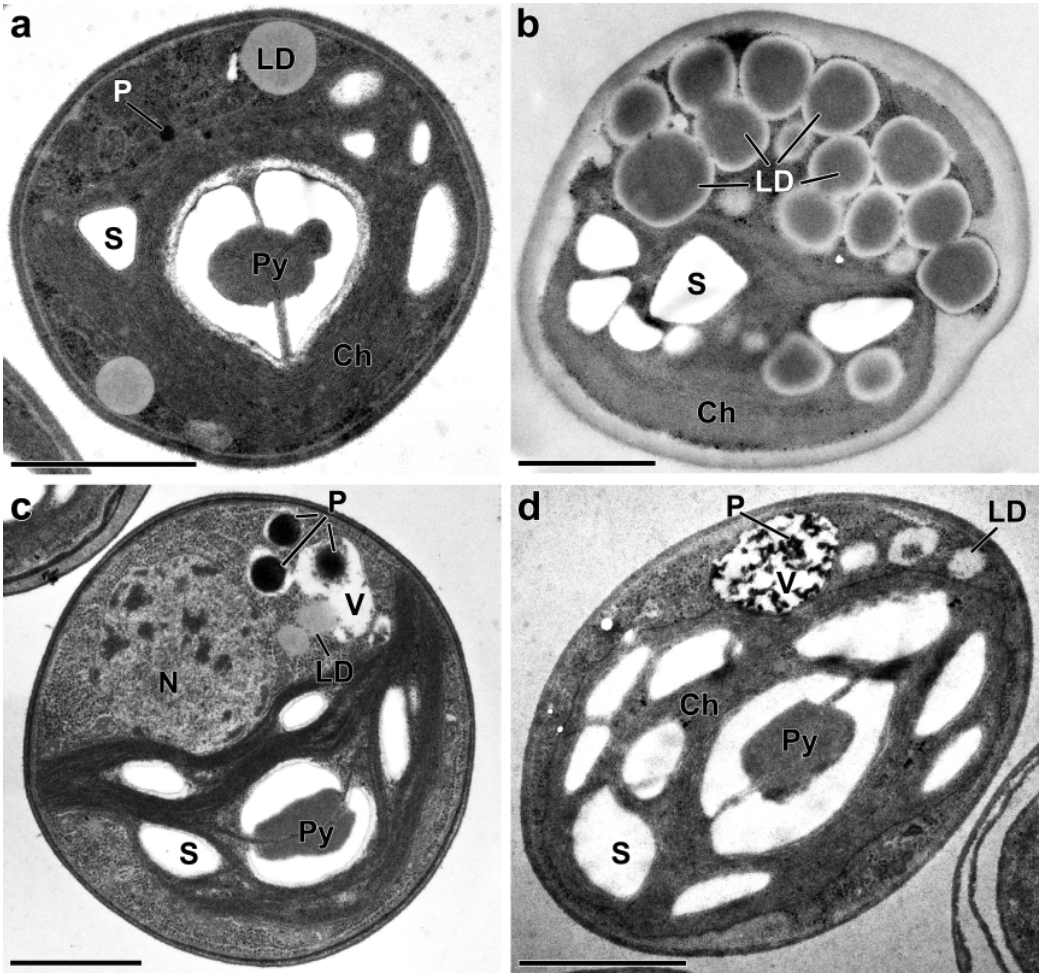

Fig. 3. The ultrastructure of *Chlorella vulgaris* IPPAS C-1 cells from (a) the pre-culture grown in the P-replete media, (b) the culture grown 17 d in the P-free medium, the culture grown after P replenishment of P_i in the medium (c) 5 d and 11 d (stationary-phase). Ch, chloroplast; LD, lipid droplet(s); P, vacuolar PolyP granules, Py, pyrenoid; S, starch grain; V, vacuoles with granules. Scale bars: 1 μm.

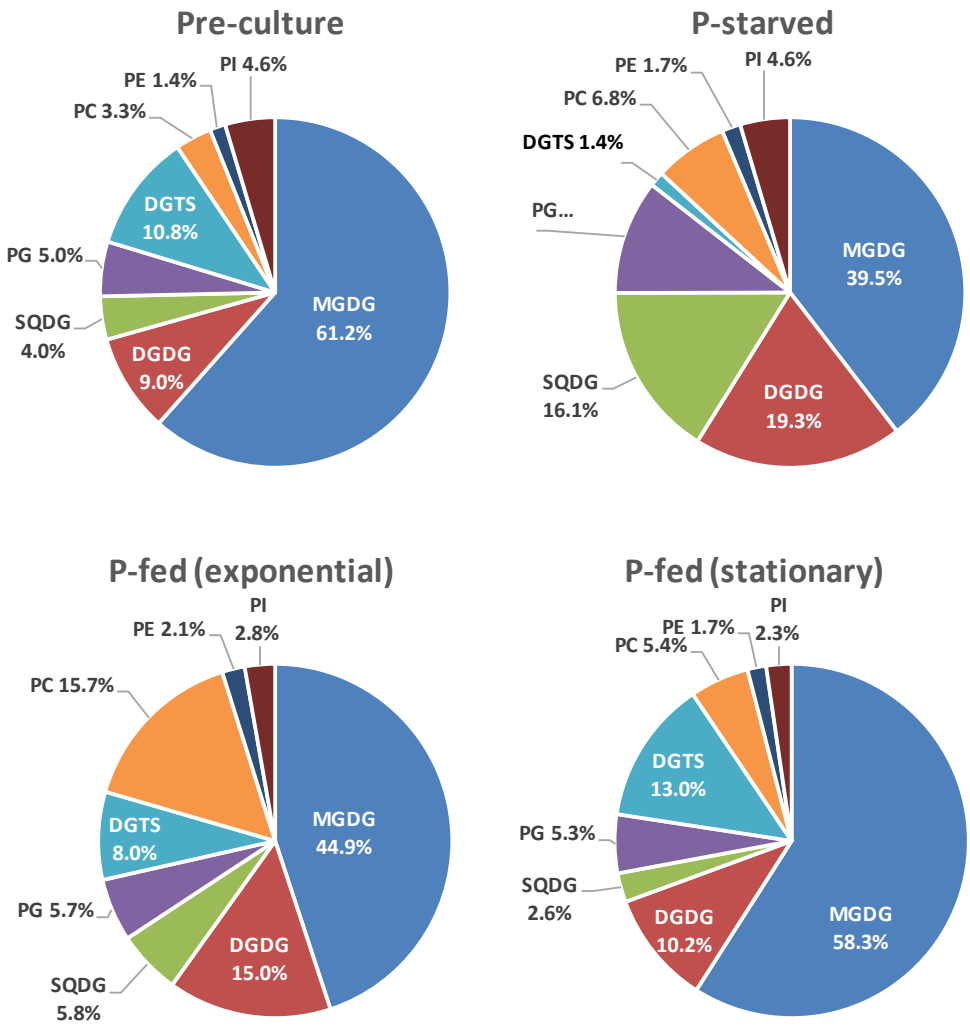

Fig. 4. Composition of lipid classes in *Chlorella vulgaris* IPPAS C-1 cell from P-sufficient precultures, P-starved cells as well as of the cells from the cultures exponentially growing and reaching stationary phase after re-feeding. MGDG, Monogalactosyldiacylglycerols; DGDG, digalactosyldiacylglycerols; SQDG, sulfoquinovosildiacylglycerol; PG, phosphatydilglycerol; DGTS, diacylglycerylatrimethylhomoserine; PC, phosphatyldilcholine; PE, phosphatydilethanolamine; PI, phoisphatydilinosytol.

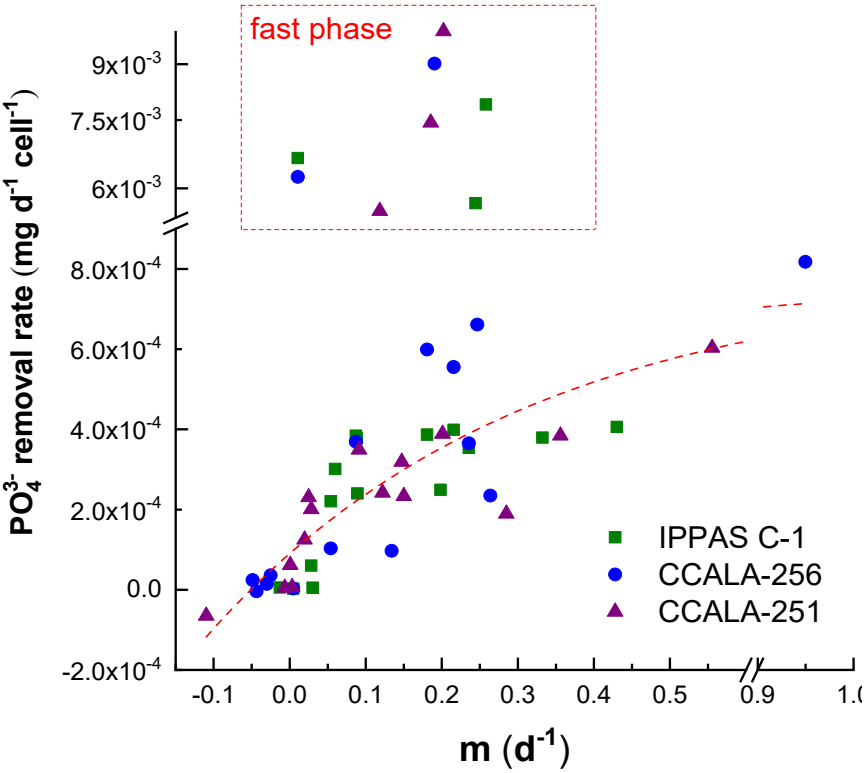

Fig. 5. Relationships between the specific growth rate, μ, and P_i uptake rate after re-feeding of the P pre-starved cells of *Chlorella* strains during fast P_i uptake phase (0-240 min after P_i addition; dashed frame) and during slow P*i* uptake phase (1–7 d after P_i addition).

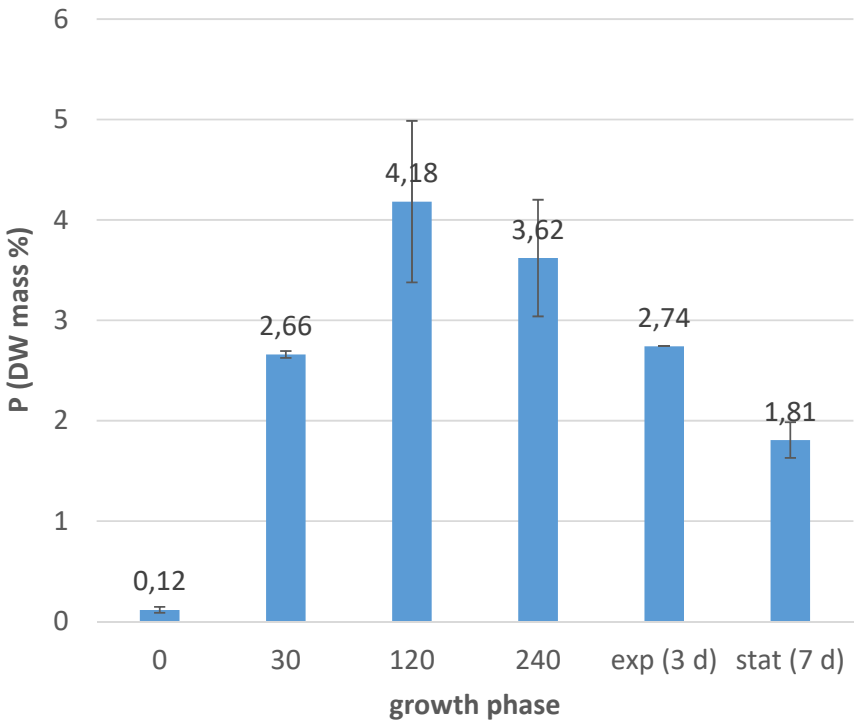

Fig. 6. Total P content of the *C. vulgaris* IPPAS C-1 cells before and after their re-feeding with P_i as a function of time after re-feeding and the culture growth phase (lag phase, 0–240 min; logarithmic phase, 3 d; and stationary phase, 7 d).

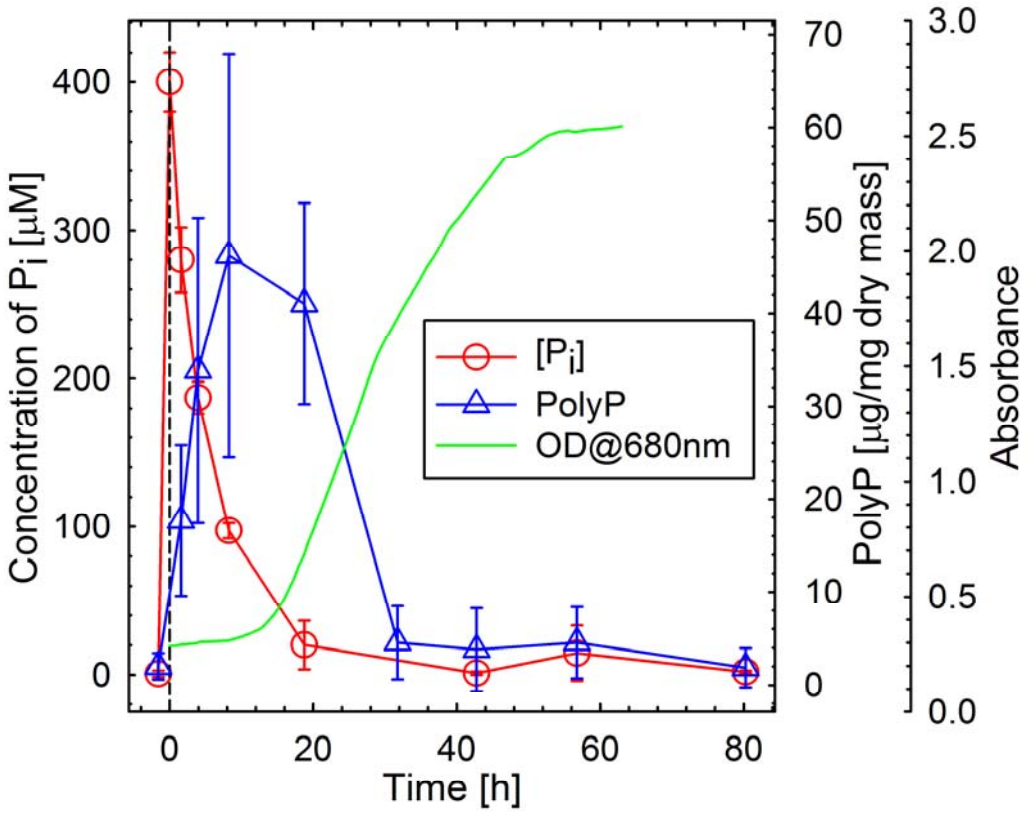

Fig. 7. Kinetics of the PolyP content detectable by Raman microscopy inside intact cells of *Chlorella vulgaris* CCALA-256 (blue line, triangles) after replenishment of P_i to 400 μM. The moment of replenishment is indicated by a vertical dash line. The time evolution of intracellular PolyP content is correlated with the P_i concentration remaining in the medium (red line, circles) and growth of the culture expressed as absorbance at 680 nm (green line).

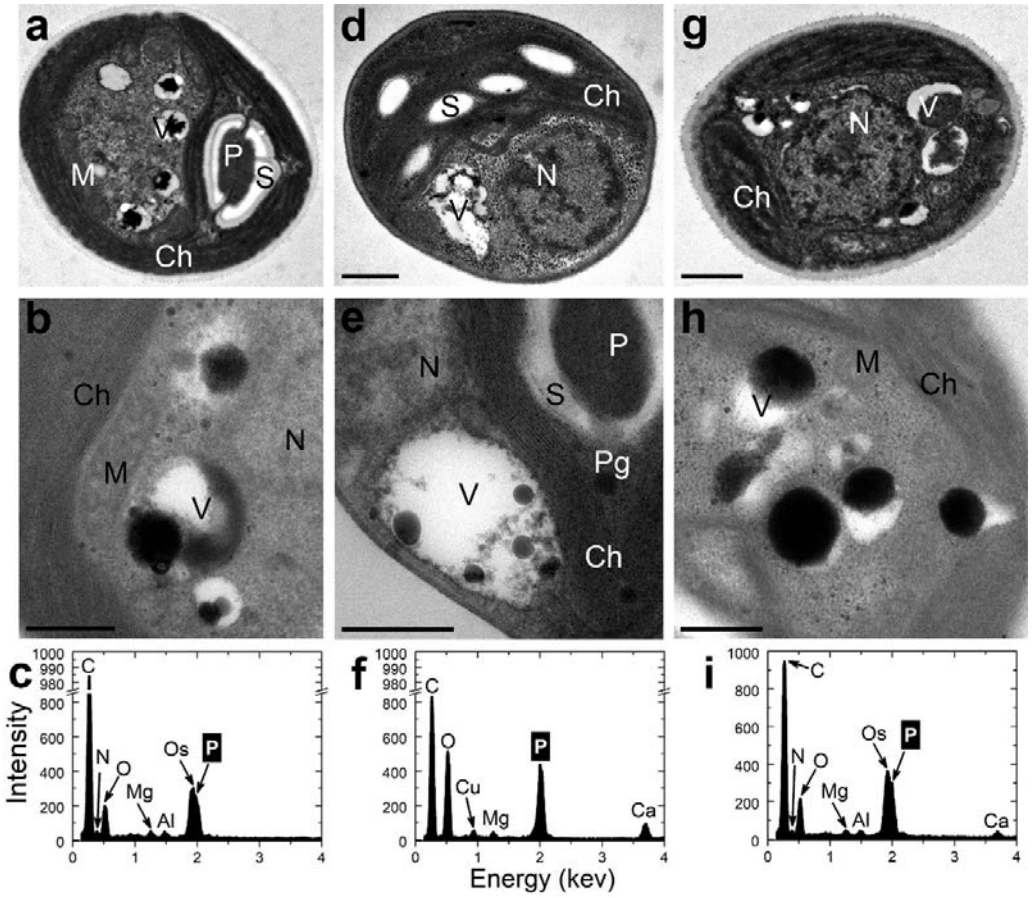

Fig. 8. Polyphosphate accumulation in the cells of (a-c) *C. vulgaris* CCALA 256, (d-f) *C. vulgaris* IPPAS C1 and (g-i) *P. kessleri* CCALA 251. (a, d, g) TEM images of ultrathin sections through the central region of the cell. (b, e, h) TEM image of semi-thin sections of the cells with putative polyphosphate granules in the vacuoles. (c, f, i) The point (30 nm^2) EDX spectra of the granules containing the characteristic peaks of P. Ch, chloroplast; M, mitochondrion; N, nucleus; P, pyrenoid; Pg, plastoglobuli; S, starch grain; V, vacuole. Scale bars: 0.5 µm.

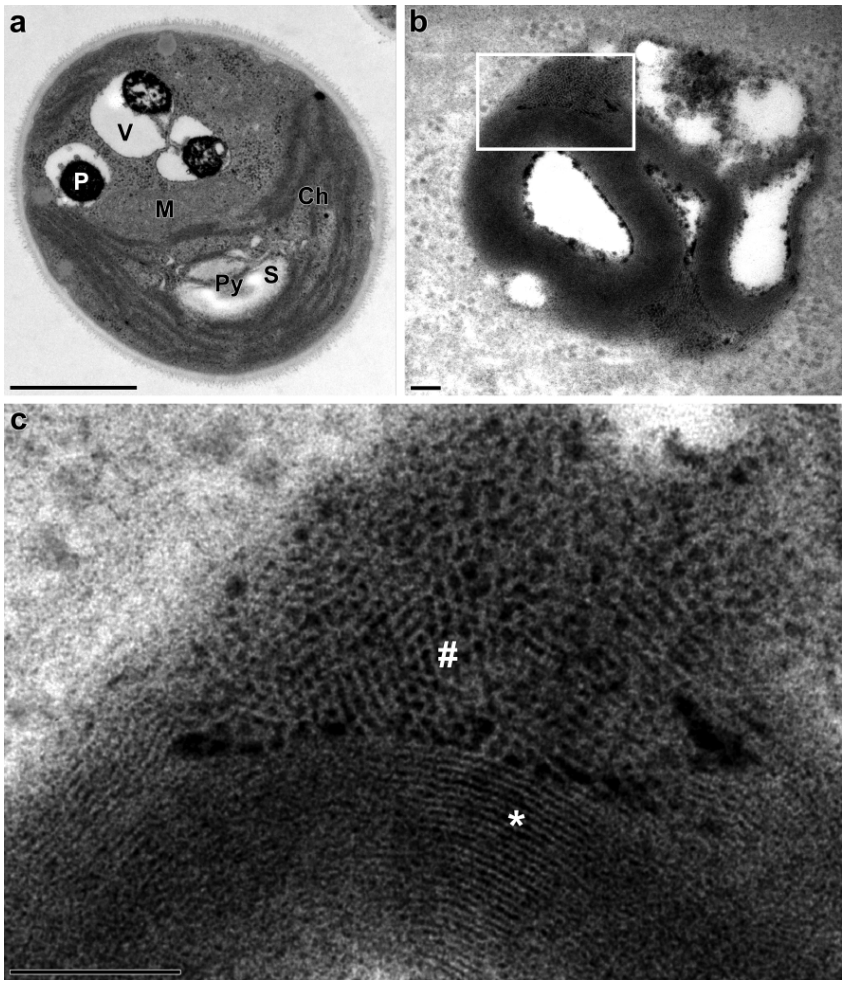

Fig. 9. The ultrastructure of *Chlorella vulgaris* CCALA 256 cells with the vacuolar PolyP granules from stationary-phase (9 d from P re-feeding) culture: (a) survey micrograph view of the cells, (b) TEM image of the PolyP granule in the vacuole and (c) its enlarged fragment. Ch, chloroplast; M, mitochondrion; P, PolyP granule, Py, pyrenoid; S, starch grain; V, vacuoles with granules. In (c), the longitudinal-cut (asterisk) and (#) cross-cut regions of the "multi-wire cable" chains of the electron-dense particles are shown (see also Fig. 10). Scale bars: 1 µm (a) and 0.1 µm (b, c). (b) and (c) adapted from [69] with kind permission of Springer.

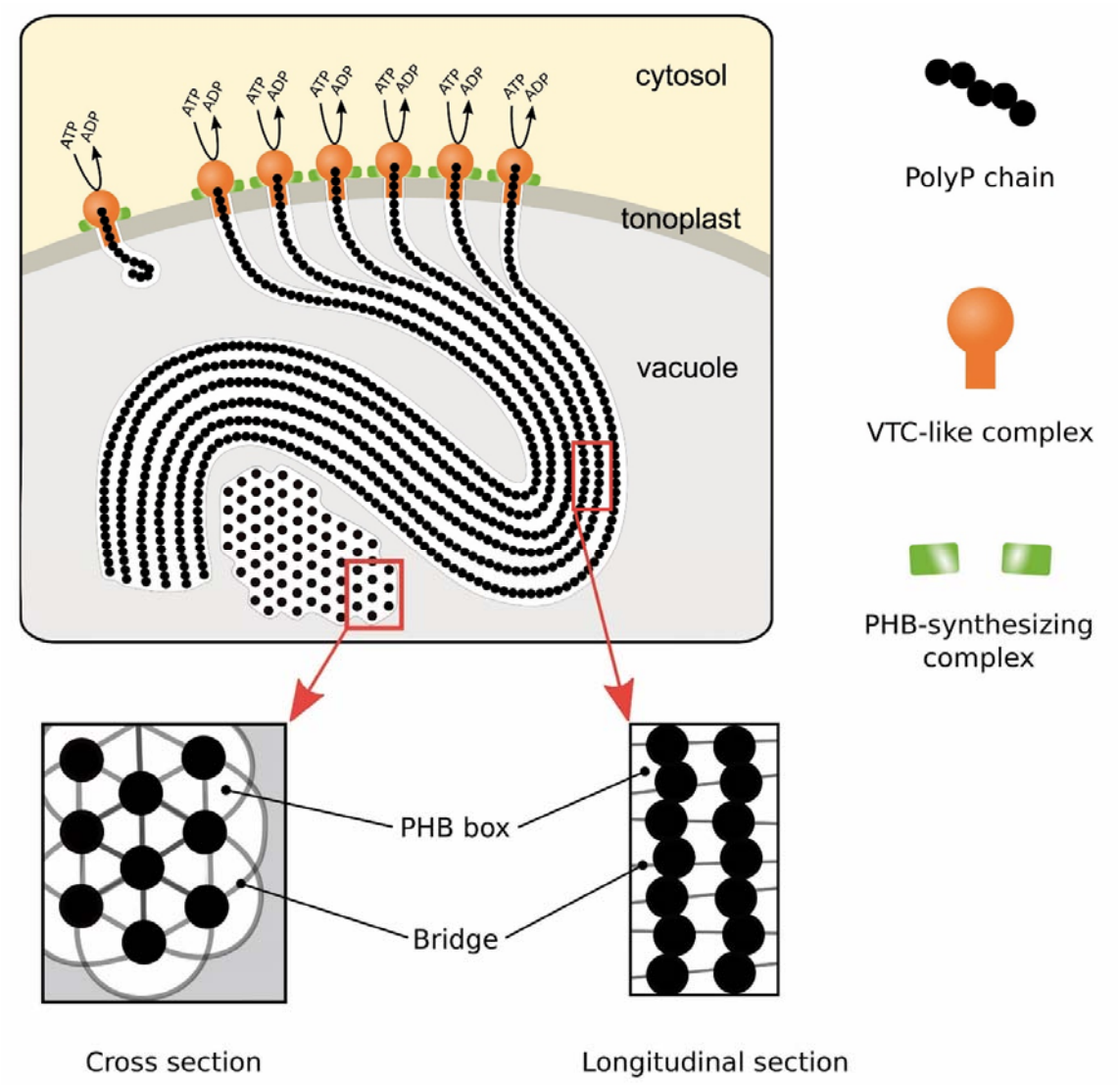

Fig. 10. A hypothetical schematic representation of the coupled biosynthesis of the PolyP chains and its transportation into the vacuole by the tonoplast-bound VTC-like enzyme complexes leading to the formation of the P-rich inclusions displaying. The ends of the PolyP chain are likely sealed with bridge-like structures composed by poly-(R)-3-hydroxybutirate (PHB). The "multiwire cable" ultrastructural pattern arises likely from the simultaneous operation of many VTC-like complexes organized as raft(s) floating in the tonoplast.

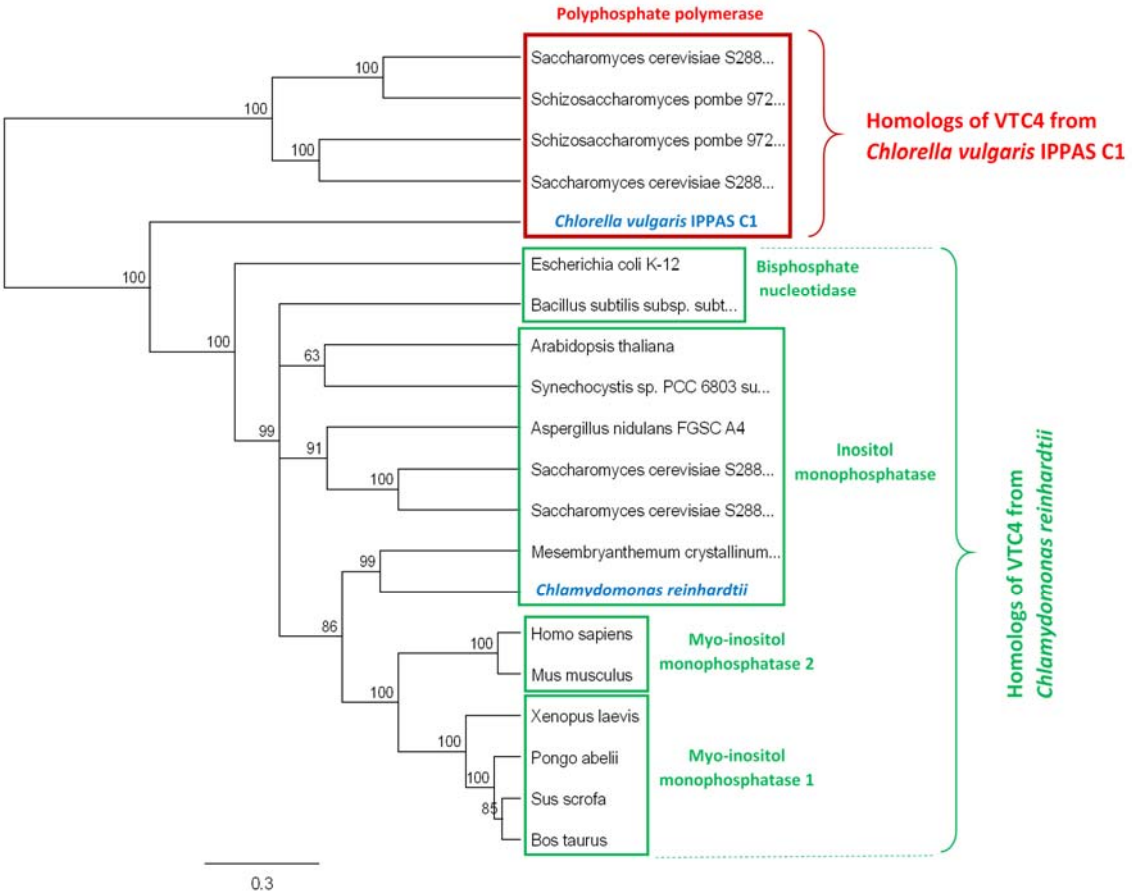

Fig. 11. Phylogenetic relationships between VTC-like proteins from different organisms (note the ubiquity of corresponding enzymes in species from very distant taxa) with diverse functions in the cell. Closest homologs of VTC4-like protein are the yeast polyphosphate polymerases from the same family. The similarly annotated protein in *Chlamydomonas reinhardtii* is similar to a different enzyme family (also present in yeast).

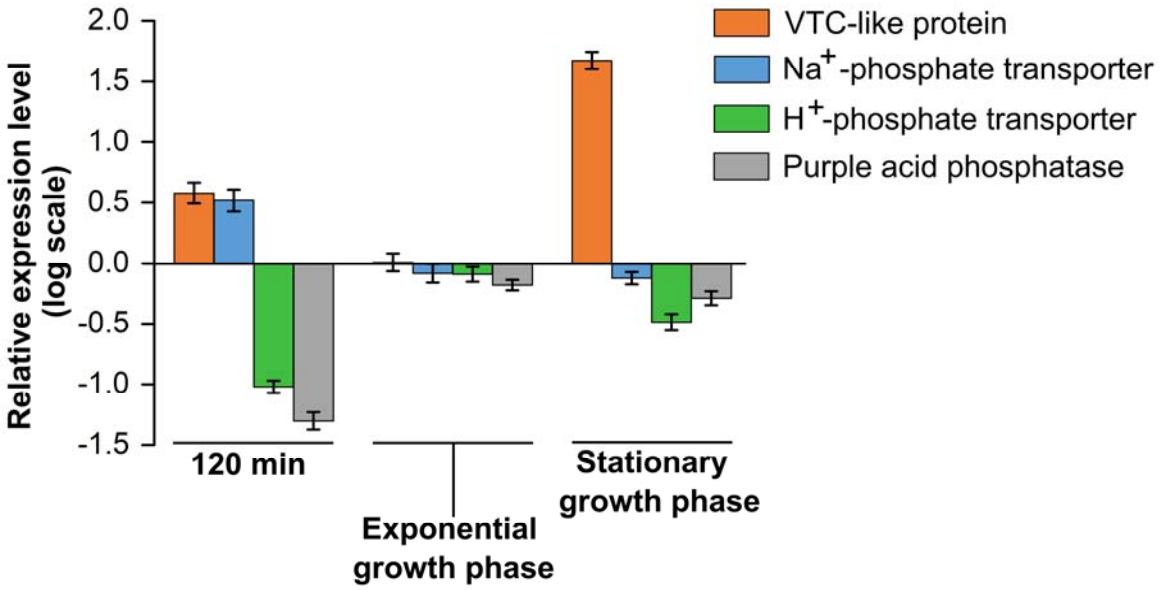

Fig. 12. Changes in the expression levels of the genes putatively involved in P_i uptake and metabolism of PolyP after re-feeding of P-starved cells of *Chlorella vulgaris* IPPAS C-1 relatively to the level typical for P-starved cells and normalized to the expression of the ubiquitinligase E3. Average values of two biological replications are shown, each with two technical replicas (n = 4) ± SE.

Supplementary material

Table S1. Selected JIP-test parameters used in this work [92].

Fo, Fm, Fm'	Fluorescence intensity at the point O and at the point of the maximum of OJIP (m) in dark-adapted state. Fm' represents Fm in light-adapted state.
$Q_y = \frac{\mathrm{Fm} - \mathrm{Fo}}{\mathrm{Fm}} = \frac{\mathrm{Fv}}{\mathrm{Fm}}$	Maximum photochemical quantum yield of photosystem II in dark-adapted state; represents the potential for absorbed photon energy transduction into electron transport.
$\mathrm{NPQ} = \frac{\mathrm{Fm}}{\mathrm{Fm'}} - 1$	Stern-Volmer non-photochemical quenching.

Table S2. The primers for rtPCR used in this work.

Name	Sequence (5'-3')	Putative protein (domain) encoded
Ref_for	TAGAGGATTCCGAGGACATCTG	Ubiqutinligase E3
Ref_rev	CAGGTGGAAGTGGTGGTTG	
VTC_for	ATCATTCGCTTCCCGTACG	Vacuolar transport chaperone, VTC
VTC_rev	AGGAACTTGGAGAACTTGGG	
Trans1_for	AAGGCGCTGACGATGAAG	Na^+/P_i-symporter
Trans1_rev	AAGATGTCTGGGTCATTCACG	
Trans2_for	ACATCCTGCTTAACAACGGG	H^+/P_i-symporter
Trans2_rev	CAGGAAGAGTAGGAAGAGCATG	
Phosph_for	TCCTATGCTGACCTCTACTACTC	Purple acidic phosphatase
Phosph_rev	TTCCCTGGCACAAAGACTG	

Supplementary Methods

RNA isolation

For the transcriptome sequencing total RNA from the *C. vulgaris* IPPAS C-1 cells was isolated with RNeasy Kit (Qiagen, Germany) according to the manufacturer's protocol. Cells resuspended in the lysis buffer (Buffer RLT) and homogenized in a TissueLyser II homogenizer (Qiagen, Germany). After the extraction, RNA quality was checked using capillary electrophoresis on Bioanalyser 2100 (Agilent, Santa-Clara, USA). The isolated RNA was stored at –70°C.

For the real-time PCR, total RNA was isolated from C vulgaris C-1 cells with RNeasy Plus Mini Kit (Qiagen, Germany). The cells samples (approximately 1×10^7 cells) were precipitated by centrifugation (3000 × *g*, 2 min), resuspended in 600 µl of the lysis buffer (Buffer RLT Plus) and placed into 2 ml FastPrep® tubes to destroy the cells with the lysing matrix B (MP Biomedicals, LLC, USA) in the Fastprep-24™ 5g homogenizer (MP Biomedicals, LLC, USA). The cell lysate was clarified by centrifugation (8000 × *g*, 5 min) and transferred to the centrifuge column to remove genomic DNA (gDNA Eliminator spin column) from the specified kit. The procedure of RNA isolation was continued according to the protocol of the manufacturer. The obtained RNA preparations were stored at –70°C.

Transcriptome assembly and analysis

Prior to cDNA library construction, polyA-mRNA fraction was selected using oligo-dT magnetic beads (Illumina, San-Diego, CA, USA) and processed using NextFlex Rapid Directional RNA-Seq Kit (Bioo Scientific, Austin, TX, USA).

cDNA libraries were quantified using Qubit 1.0 fluorometer (Invitrogen, Carlsbad, CA, USA) and quantitative PCR, diluted to 10 pM and sequenced using HiSeq2000 instrument from both ends of the fragment (read length = 100 nt) with TruSeq v.3 sequencing chemistry (Illumina, San-Diego, CA, USA). Raw data were processed with CASAVA v. 1.8.2. Assembly was performed using CLC genomics Workbench with following parameters: word size = 64, bubble size = 50, minimum contig length = 300.

The contigs were annotated according to molecular function, biological process, and cellular component by Blast2GO (www.blast2go.com) v3.0 InterPro [42] scan with Nr and Pfam annotation [43] in Gene Ontology (GO) database (http://geneontology.org/), and at Kyoto Encyclopedia of Genes and Genomes Pathway database (KEGG, http://www.genome.jp/kegg/) Automatic Annotation Server.

To reveal protein structures evolutionary related to the putative sequences of the selected proteins found at the previous step, the SWISS-MODEL template library (SMTL version 2015-09-09, PDB release 2015-09-04) [93] was searched with BLAST [44] and HHBlits [94].

Homologous sequences were searched against NCBI GeneBank (nucleotide collection nr/nt database) using BLAST (http://blast.ncbi.nlm.nih.gov/) [44]. Sequence data analysis, including multiple alignments, was conducted in Geneious v8.6 (www.biomatters.com) using Tamura-Nei DNA evolution model [95] and MUSCLE algorithm [96] with default parameters. Phylogenetic tree was constructed using Geneious Tree Builder and UPGMA algorithm [97] with

default parameters. The accuracy of the tree topology was tested using bootstrap analysis [98] with 100 replicates.

Real-time PCR

Synthesis of the single-strand cDNA for real-time PCR (RT-PCR) was performed using QuantiTect Reverse Transcription Kit (Qiagen, Germany) according to the manufacturer's protocol. Approximately 250 ng RNA was taken for each sample in the cDNA synthesis reaction.

Primers were designed using the RealTime PCR Tool (Integrated DNA Technologies, Inc., https://eu.idtdna.com/scitools/Applications/RealTimePCR/) with the default parameters for the contigs putatively associated with the genes involved in the P_i transport, metabolism of polyphosphates, and the gene of endogenous control (see Table S2 and Figs. S3- S7). The RT-PCR targets were selected after analysis of the de novo assembled transcriptome of *C. vulgaris* C-1 based on the annotation of the contigs in the assembly, and the alignment of sequences with known genes of other microorganisms with the target function. All primers used in the work for PCR in real time during amplification gave reaction efficiency ≥90% and led to the formation of a product with a single peak on the melting curve.

The search for the nearest homologous sequences to the identified contigs was performed in the database of nucleotide sequences of NCBI GeneBank using the BLAST software [44]. Multiple sequence alignment and construction of phylogenetic trees was carried out in the program Geneious v9.0 (Biomatters Ltd, New Zealand) using the built-in in the program Geneious Alignment of the model with the default settings.

Real-time PCR was performed using the QuantiTect SYBR Green PCR Kit (Qiagen, Germany) according to the manufacturer's recommendations, the QuantStudio 7 Flex Real-time PCR System (Thermo Fisher Scientific, USA) and the Applied Biosystems QuantStudio™ Real-time PCR Software Version 1.3 (Thermo Fisher Scientific, USA).

Each reaction mixture (10 µl) contained 0.25 µl of each primer with a concentration of 10 µm (direct and reverse, the final concentration in the mixture of each 0.25 µm); 5 µl of a buffer with a fluorescent dye SYBR Green QuantiTect SYBR Green PCR Master Mix containing HS-Taq DNA polymerase from this kit; 1 µl of cDNA obtained in the reaction of cDNA synthesis on the RNA matrix and diluted 25 times (reaction with primers REF1, VTC, trans2) or 5 times (REF1, trans5, pho1, pho2); 3.5 µl of RNAse-free water.

Immediately prior to the reaction, the reaction mixture was pre-heated to activate HS-Taq-DNA polymerase (95°C, 15 min). The reaction included 35 cycles, each cycle consisted of DNA denaturation (94°C, 15 C), primer annealing (58°C, 30 C) and DNA chain synthesis (72°C, 30 C). After the reaction, the melting curves of the amplification products were obtained. Controls without the template and reverse transcriptase were included.

All measurements were carried out with two biological and two analytical replicas. The expression of the target genes at different stages after re-feeding was calculated relatively to that recorded in the P-starved cells. The obtained data were processed using the Thermo Fisher Cloud Data Analysis software (Thermo Fisher Scientific, USA) with the default parameters at which gene expression was calculated by the formula $\Delta = 2^{-(C_t - C_t^0)}$, where Δ is the differential gene expression level, C_t is the cycle number at which the fluorescence signal from the sample in question crosses the baseline, C_t^0 is the cycle number at which the fluorescence signal from the P-starved cell sample crosses the baseline.

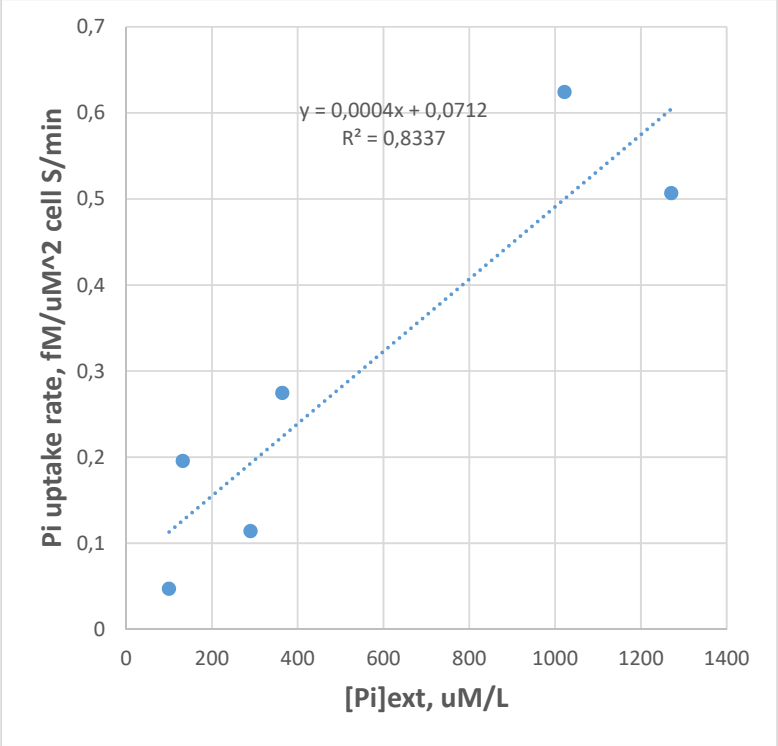

Fig S1. Dependence of the rate of P_i uptake by the P-starved cells of *C. vulgaris* IPPAS C-1 on the concentration of P_i added during their P re-feeding.

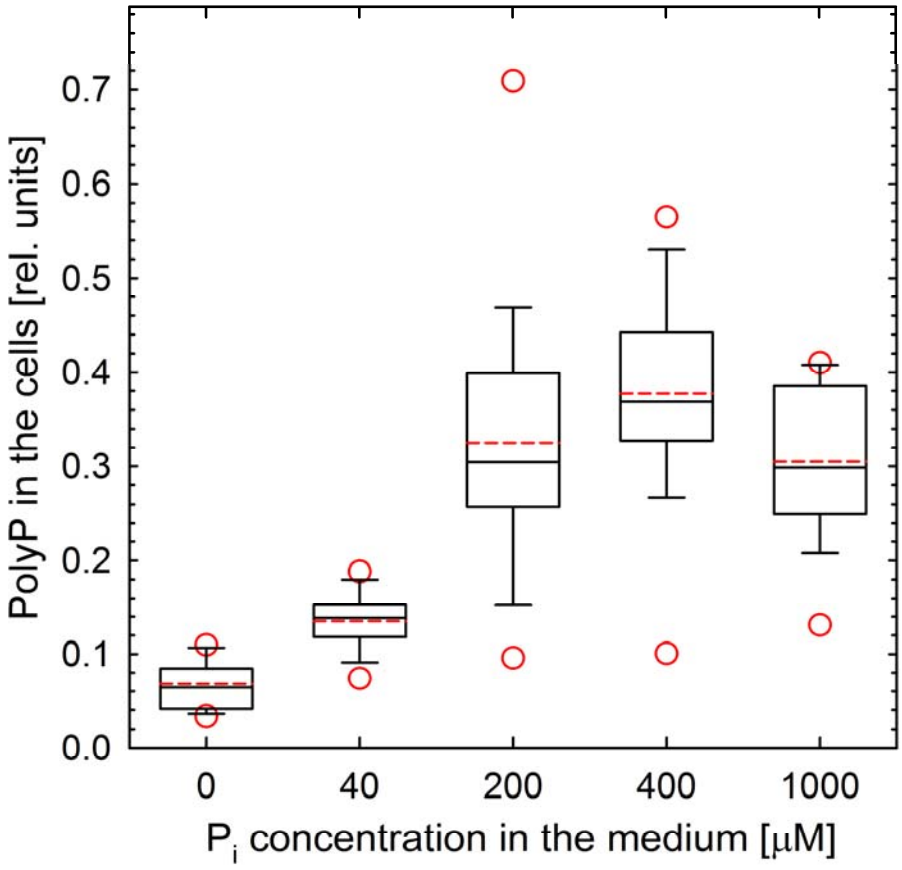

Fig S2. Relative content of PolyP detectable by Raman microscopy in algal cell as a function of P_i concentration (0–1000 μM) replenished to the medium. First cell of each sample was measured 100 min after the P_i replenishment. In addition to the box-and-whiskers presentations of quartiles, means and outliers are shown in red. Each sample consisted of ca 30 cells.

Table S3. The occurrence of the characteristic "multi-wire cable" ultrastructural pattern of PolyP in microalgal cells.

Organism	Growth medium	Time after re-feeding/growth phase	Subcellular localization
Chlorella vulgaris IPPAS C-1	BG-11	8 h/lag	Vacuole*
Parachlorella kessleri CCALA 251	BG-11	7 d/stat	Vacuole
Chlorella vulgaris CCALA 256	BG-11	7 d/stat	Vacuole**
Lobosphaera incisa SAG 2468	BG-11m	3 d/exp	Vacuole
	BG-11 -P	3 d/stat	Vacuole*
Desmodesmus sp. IPPAS S-2014	BG-11	3 d/exp	Vacuole*

*There were also some grains in cytosol in tight contact with vacuole and, scarcely, in the chloroplast stroma.

**In tight contact with nuclear envelope or between the nuclear membranes.

Table S4. Differentially expressed genes involved in P_i uptake and PolyP biosynthesis (FDR < 0.05) in *Chlorella vulgaris* IPPAS C-1 exposed to P starvation with subsequent re-feeding. Data for the cell samples taken at 30, 60, 120, 180, 300 min after re-feeding as well as at logarithmic and early stationary phase (3 d and 7 d after re-feeding, respectively) are shown. Data are expressed as fold-changes relative to the P-starved cells; only significant data are shown (p < 0.05).

GenBank ID	Transcript ID	Functional annotation	Change of expression level, logFC						
			30′	60′	120′	180′	300′	3d	7d
MK334249	cv11806	VTC2/VTC4-like	2.26	0.15	1.24	1.15	1.34	1.38	4.14
MK334251	cv17861	H^+/P_i symporter	-4.63	-2.53	-1.13	-0.39	0.18	1.61	0.49
MK334252	cv11978	Na^+/P_i symporter (*Pho4*/*PitA*-like)	-0.72	-1.97	-1.35	-2.68	-3.17	-2.38	-4.60
MK334253	cv12459	Purple acid phosphatase	-2.00	-1.67	-1.08	-0.25	0.18	0.50	-0.93

Organism	Designation	GenBank/ Phytozome ID	a.a. numbers	% identity to Cvu
Chlorella vulgaris IPPAS C-1	Cvu	MK334250	32–88	N/A
C. sorokiniana	Cs	PRW57997.1	168–224	98
Micractinium conductrix	Mc	PSC75162.1	147–203	81
C. variabilis	Cva	XP_005847649.1	2–56	86
Lupinus angustifolius	La	XP_019452145.1	136–191	63
Tarenaya hassleriana	Th	XP_010553953.1	167–222	65
Arabidopsis thaliana	At	BAB08646.1	166–221	65
Raphanus sativus	Rs	XP_018478334.1	160–213	63
Populus euphratica	Pe	XP_011020909.1	131–186	65
Brassica rapa	Br	XP_009139814.1	160–215	65

Fig. S3. Multiple alignment of the amino acid sequences of the putative ubiquitin ligase E3 of *Chlorella vulgaris* IPPAS C-1 and the same enzyme from microalgae and plants. The conservative (interchangeable) a.a. are shaded with black (in all analyzed sequences), dark gray (n 80–100% of analyzed sequences), light-gray (in 60–80% of analyzed sequences) or white (less than in 60% of the studied sequences). The fragment of the auto-translated fragment of the putative transcript MK334250 from *C. vulgaris* IPPAS C-1 (a.a. 32–88) is shown which was used for designing of the primers for rtPCR (see Table S2).

Organism	Designation	GenBank/ Phytozome ID	a.a. numbers	% identity to Cvu
Chlorella vulgaris IPPAS C-1	Cvu	MK334249	245–289	N/A
C. variabilis	Cva	XP_005849213.1	234–279	84
Micractinium conductrix	Mc	PSC69098.1	225–270	82
Monoraphidium neglectum	Mn	XP_013900046.1	585–631	61
Auxenochlorella protothecoides	Ap	XP_011396433.1	453–498	55
Raphidocelis subcapitata	Rs	GBF99690.1	991–1037	60
Saccharomyces cerevisiae	Sc	EDV12743.1	419–468	58
Tolypocladium capitatum	Tc	PNY20637.1	425–474	58
Podospora anserina	Pa	XP_001912897.1	475–524	58
Phialophora hyalina	Ph	RDL29963.1	442–491	56

Fig. S4. Multiple alignment of the amino acid sequences of the putative VTC-like protein of *Chlorella vulgaris* IPPAS C-1 and proteins from the VTC family from microalgae and fungi. The conservative (interchangeable) a.a. are shaded with black (in all analyzed sequences), dark gray (n 80–100% of analyzed sequences), light-gray (in 60–80% of analyzed sequences) or white (less than in 60% of the studied sequences). The fragment of the auto-translated fragment of the putative transcript MK334249 from *C. vulgaris* IPPAS C-1 (a.a. 245–289) is shown which was used for designing of the primers for rtPCR (see Table S2).

Organism	Designation	GenBank/ Phytozome ID	a.a. numbers	% identity to Cvu
Chlorella vulgaris IPPAS C-1	Cvu	MK334251	30–92	N/A
C. sorokiniana	Cs	PRW32920.1	28–191	91
Micractinium conductrix	Mc	PSC76970.1	136–199	86
C. variabilis	Cva	XP_005843014.1	51–114	78
Parachlorella kessleri	Pk	BAU71130.1	45–112	77
Tetraselmis chuii	Tc	AAO47330.1	27–90	63
Volvox carteri	Vc	XP_002958976.1	4–67	61
Chlamydomonas reinhardtii	Cr	XP_001695776.1	29–93	60
Ectocarpus siliculosus	Es	CBJ33891.1	66–129	57

Fig. S5. Multiple alignment of the amino acid sequences of the putative Na^+/P_i symporter of *Chlorella vulgaris* IPPAS C-1 and those of the P_i transporters from microalgae. The conservative (interchangeable) a.a. are shaded with black (in all analyzed sequences), dark gray (n 80–100% of analyzed sequences), light-gray (in 60–80% of analyzed sequences) or white (less than in 60% of the studied sequences). The fragment of the auto-translated fragment of the putative transcript MK334251 from *C. vulgaris* IPPAS C-1 (a.a. 30–92) is shown which was used for designing of the primers for rtPCR (see Table S2).

Organism	Designation	GenBank/ Phytozome ID	a.a. numbers	% identity to Cvu
Chlorella vulgaris IPPAS C-1	Cvu	MK334252	65–127	N/A
C. sorokiniana	Cs	PRW20802.1	384–447	57
Micractinium conductrix	Mc	PSC68539.1	147–203	81
Chlamydomonas reinhardtii	Cr	XP_001701833.1	316–379	56
Chlorella variabilis	Cva	XP_005843759.1	384–447	54
Volvox carteri	Vc	XP_002955497.1	323–386	54
Monoraphidium neglectum	Mn	XP_013905031.1	163–226	51

Fig. S6. Multiple alignment of the amino acid sequences of the putative H^+/P_i symporter of *Chlorella vulgaris* IPPAS C-1 and H^+/P_i symporters of other microalgae. The conservative (interchangeable) a.a. are shaded with black (in all analyzed sequences), dark gray (n 80–100% of analyzed sequences), light-gray (in 60–80% of analyzed sequences) or white (less than in 60% of the studied sequences). The fragment of the auto-translated fragment of the putative transcript MK334252 from *C. vulgaris* IPPAS C-1 (a.a. 65–127) is shown which was used for designing of the primers for rtPCR (see Table S2).

Organism	Designation	GenBank/ Phytozome ID	a.a. numbers	% identity to Cvu
Chlorella vulgaris IPPAS C-1	Cvu	MK334253	261–323	N/A
C. sorokiniana	Cs	PRW60148.1	605–668	92
Micractinium conductrix	Mc	PSC73849.1	228–291	71
C. variabilis	Cva	XP_005845616.1	223–286	67

Fig. S7. Multiple alignment of the amino acid sequences of the putative purple acid phosphatase of *Chlorella vulgaris* IPPAS C-1 and the same enzyme from other microalgae. The conservative (interchangeable) a.a. are shaded with black (in all analyzed sequences), dark gray (n 80–100% of analyzed sequences), light-gray (in 60–80% of analyzed sequences) or white (less than in 60% of the studied sequences). The fragment of the auto-translated fragment of the putative transcript MK334249 from *C. vulgaris* IPPAS C-1 (a.a. 261–323) is shown which was used for designing of the primers for rtPCR (see Table S2).

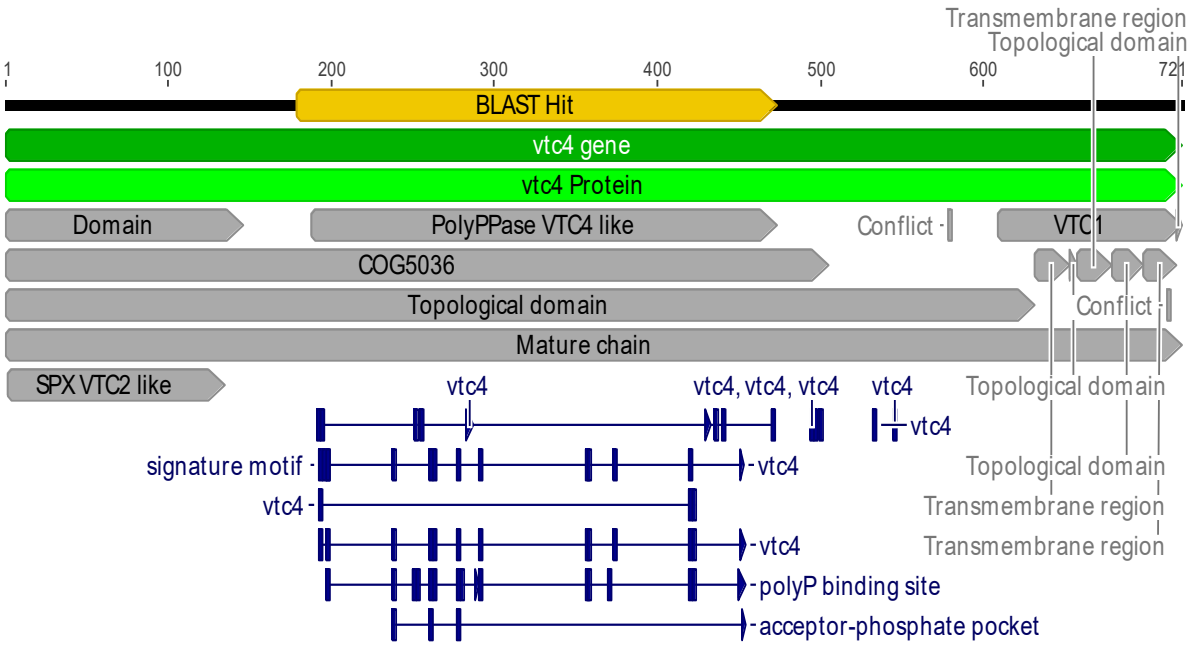

Fig. S8. Tentative functional annotation of the fragment of the transcript cv11806 encoding (a fragment of) putative VTC-like polyphosphate polymerase in *C. vulgaris* IPPAS C-1.